Gravitational Wave Astronomy (From Earth)

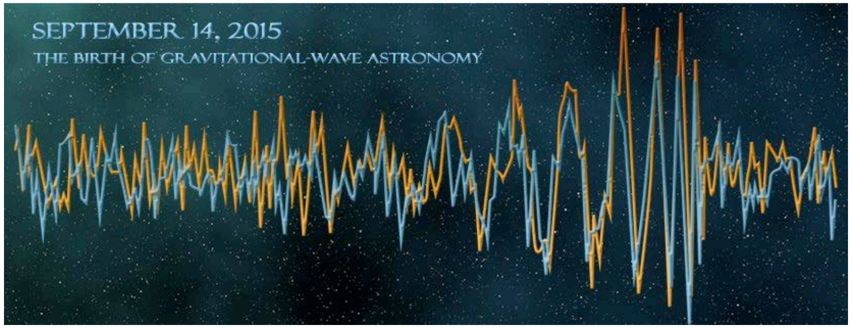

Gabriela González
Louisiana State University

(Results presented on behalf of the LIGO/Virgo/KAGRA Collaboration)

GW detectors network

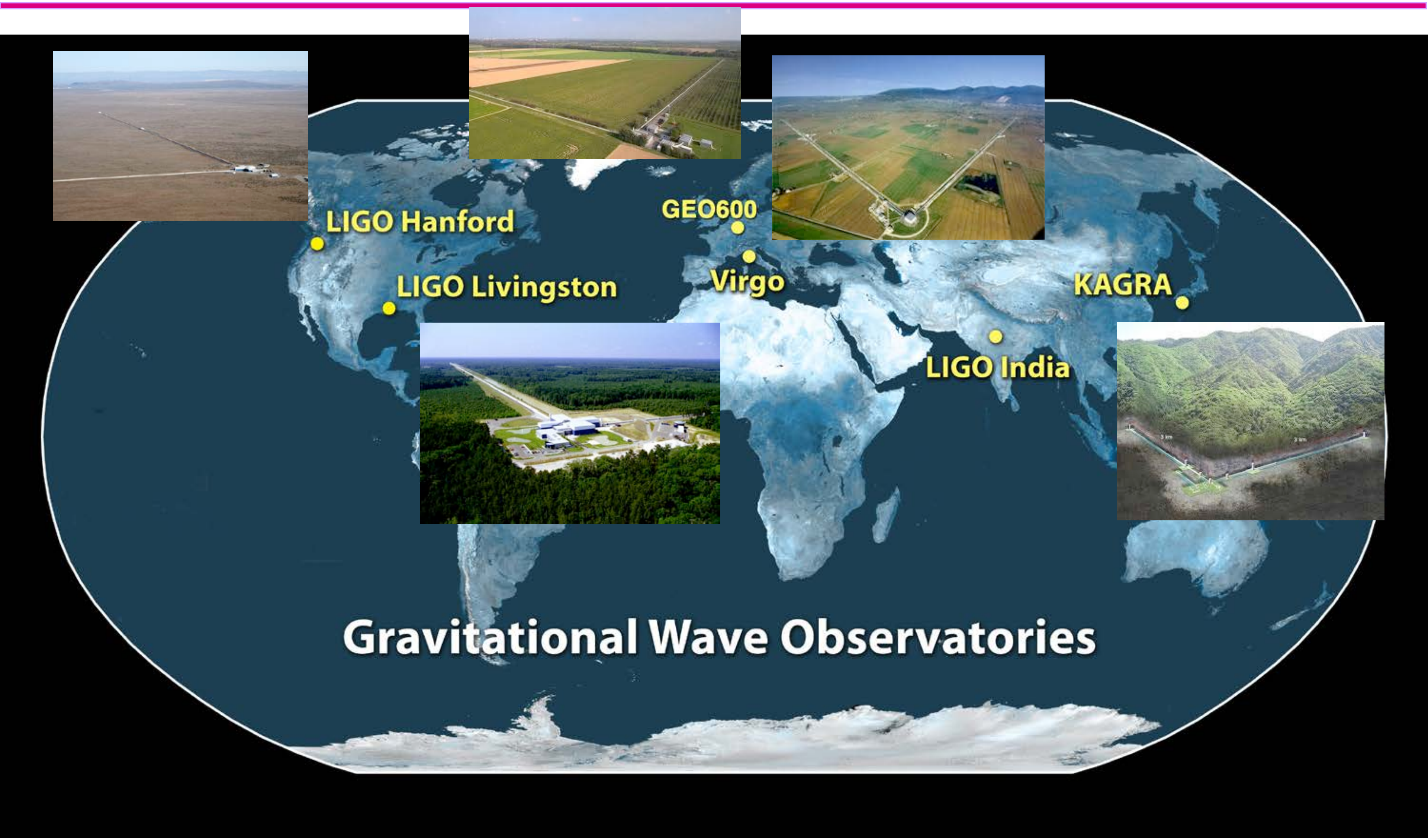

Observing Runs

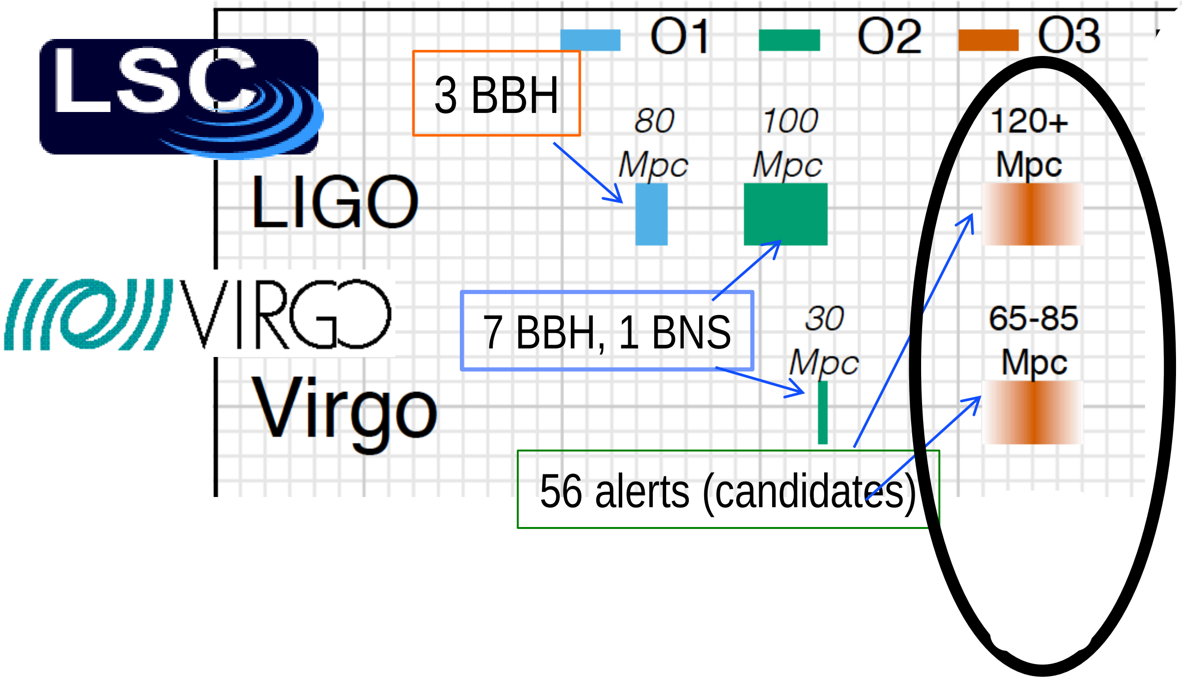

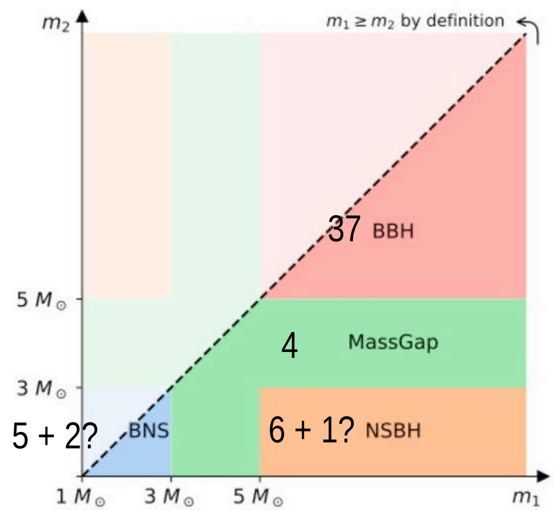

… and a (weak) different signal?

Prospects for Observing and Localizing Gravitational-Wave Transients with Advanced LIGO, Advanced Virgo and KAGRA

Living Reviews in Relativity 23, 3 (2020)

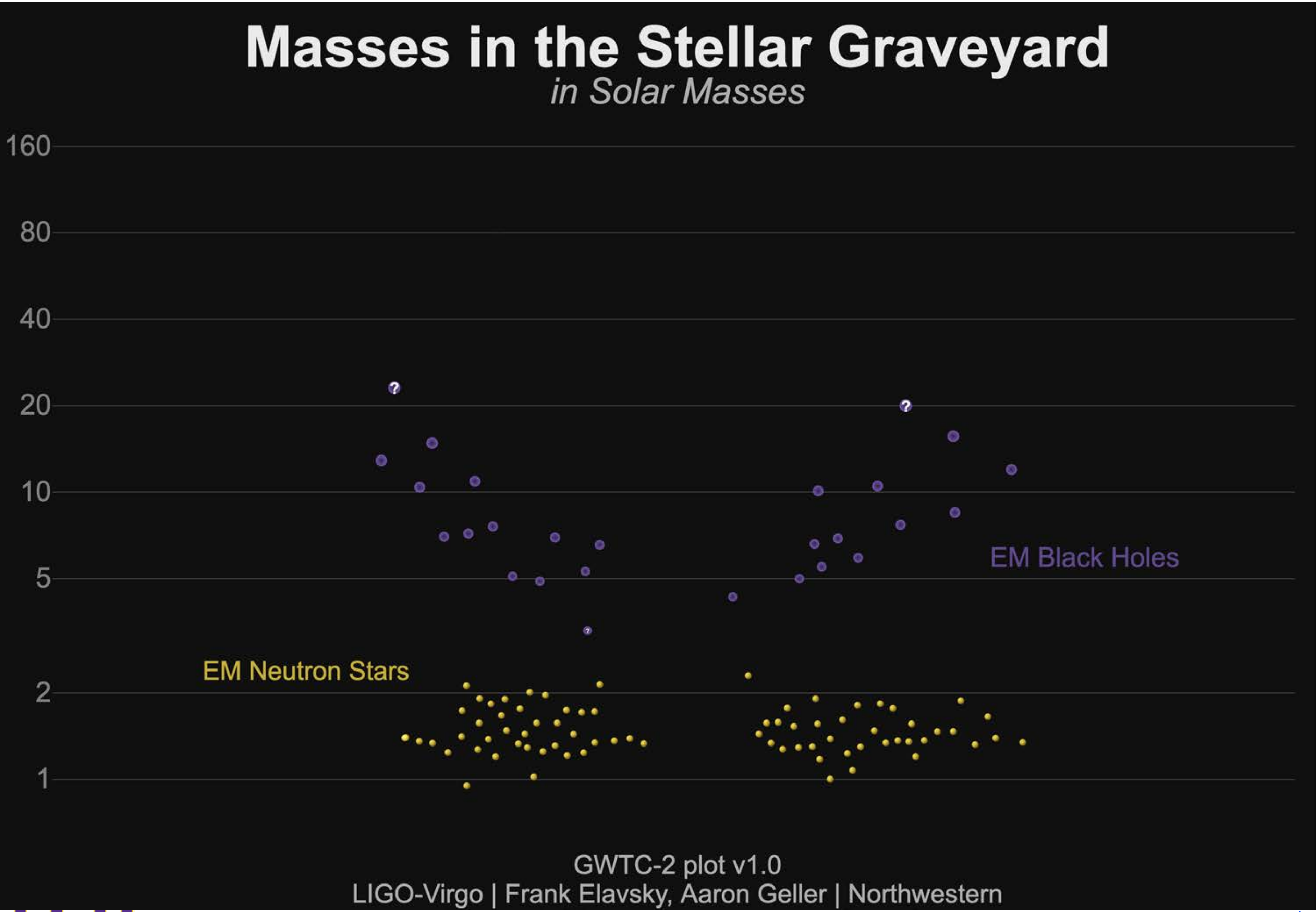
Masses in the Stellar Graveyard
in Solar Masses
160
80
40
20
10
5
2
1
EM Black Holes
EM Neutron Stars
GWTC-2 plot v1.0
LIGO-Virgo | Frank Elavsky, Aaron Geller | Northwestern

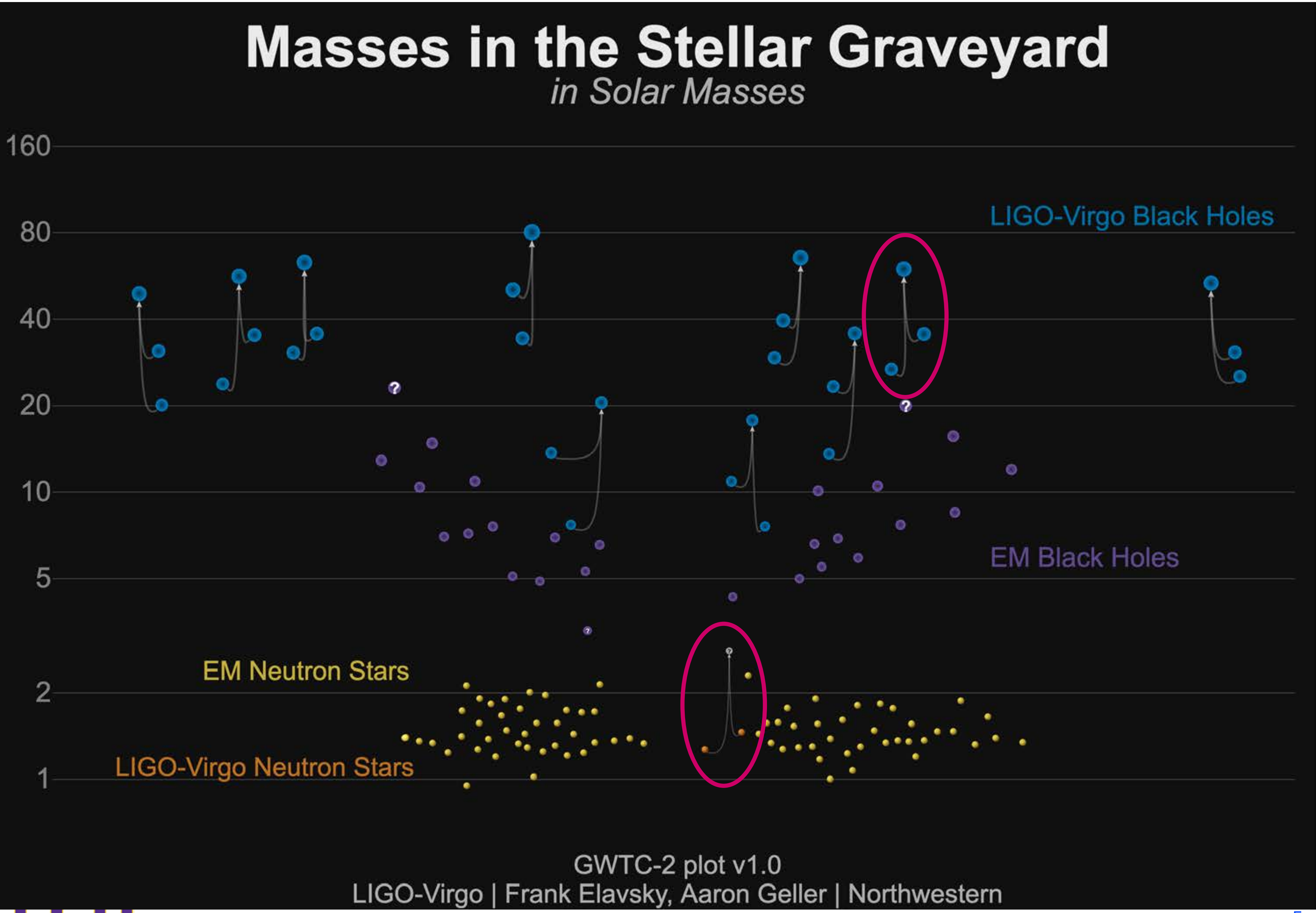
Masses in the Stellar Graveyard
in Solar Masses
160
80
40
20
10
5
2
1
LIGO-Virgo Black Holes
EM Black Holes
EM Neutron Stars
LIGO-Virgo Neutron Stars
GWTC-2 plot v1.0
LIGO-Virgo | Frank Elavsky, Aaron Geller | Northwestern

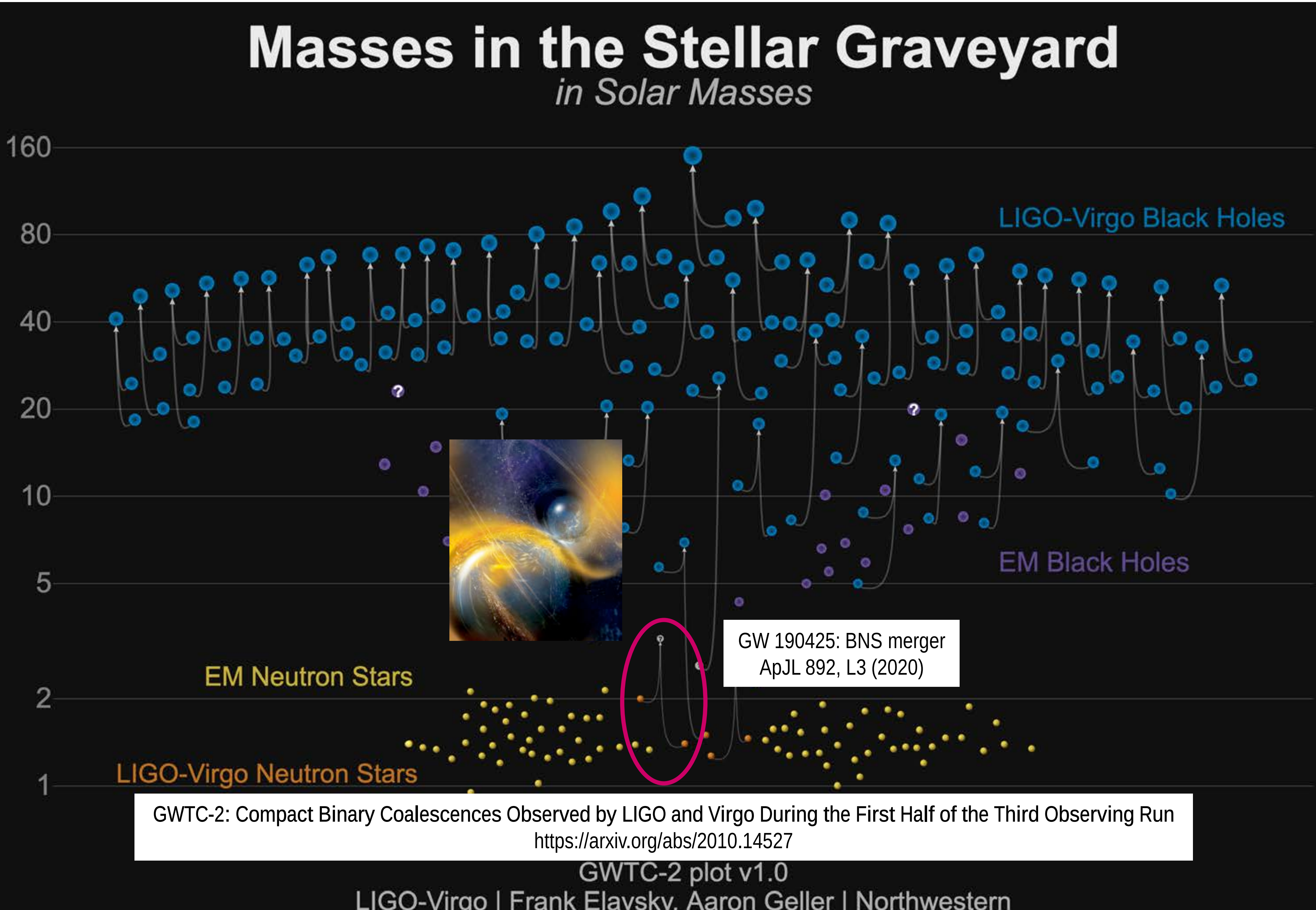

GW 190425: BNS merger
ApJL 892, L3 (2020)

GWTC-2: Compact Binary Coalescences Observed by LIGO and Virgo During the First Half of the Third Observing Run
https://arxiv.org/abs/2010.14527

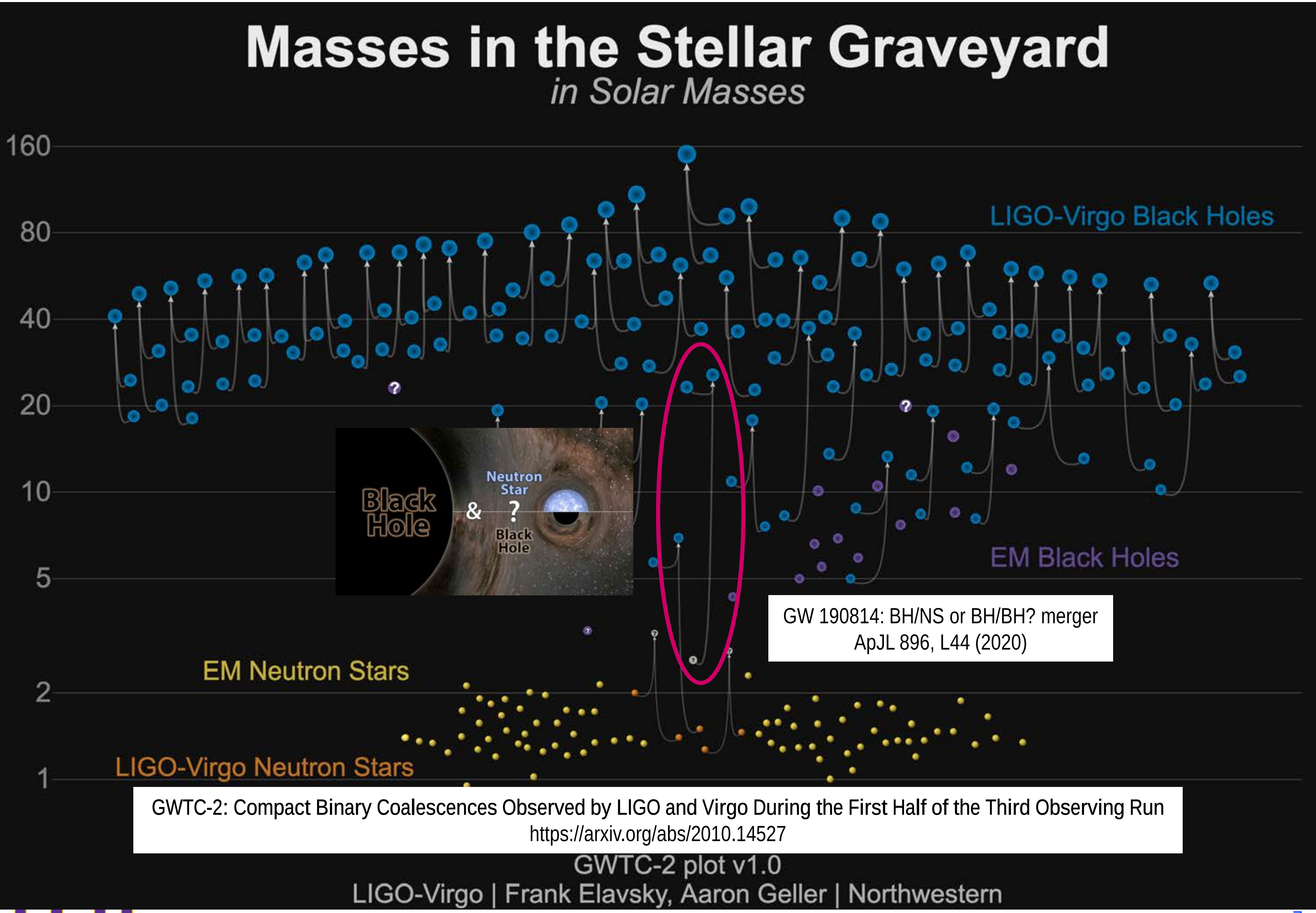

GW 190814: BH/NS or BH/BH? merger
ApJL 896, L44 (2020)

GWTC-2: Compact Binary Coalescences Observed by LIGO and Virgo During the First Half of the Third Observing Run
https://arxiv.org/abs/2010.14527

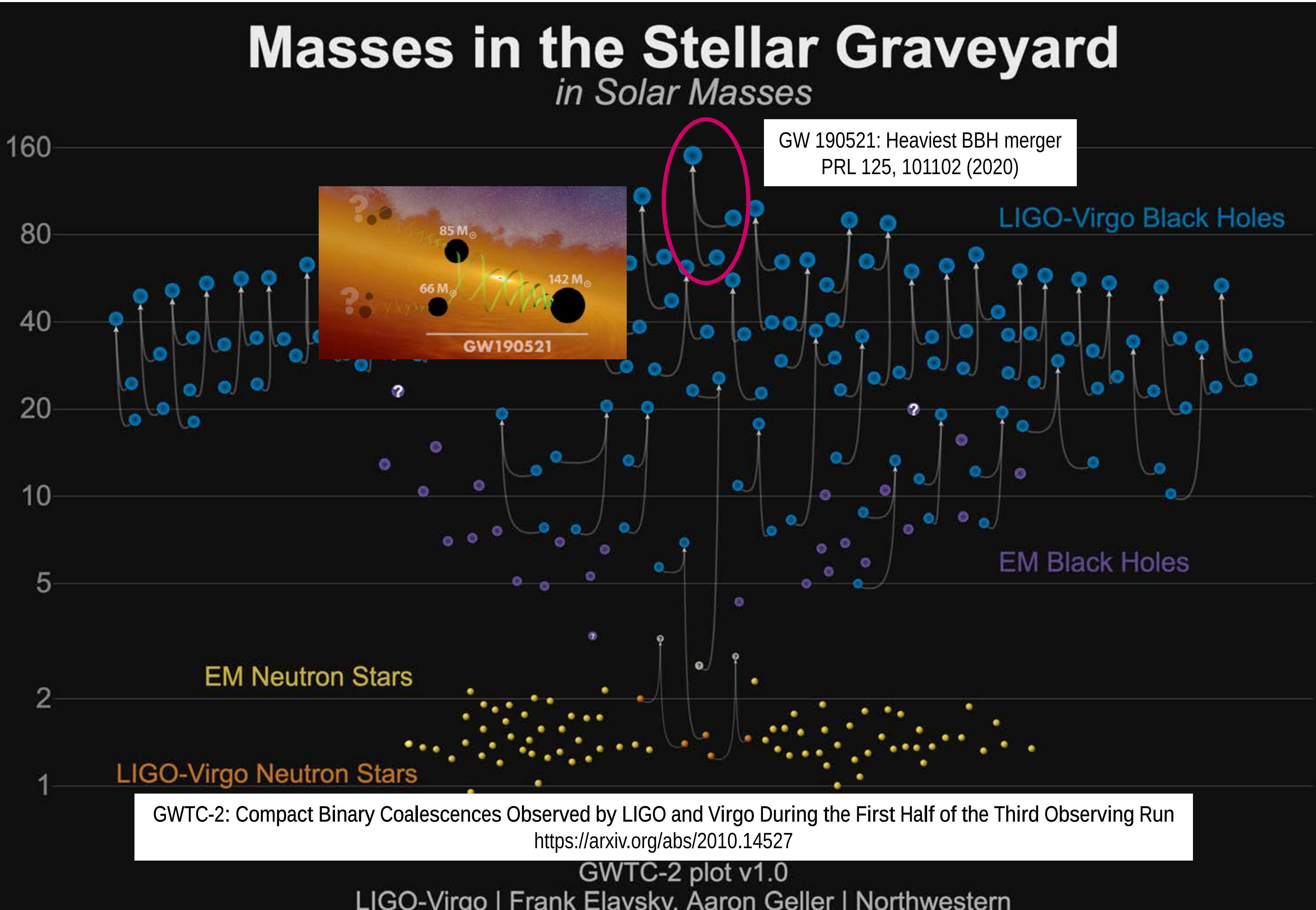

GW 190521: Heaviest BBH merger
PRL 125, 101102 (2020)

GWTC-2: Compact Binary Coalescences Observed by LIGO and Virgo During the First Half of the Third Observing Run
https://arxiv.org/abs/2010.14527

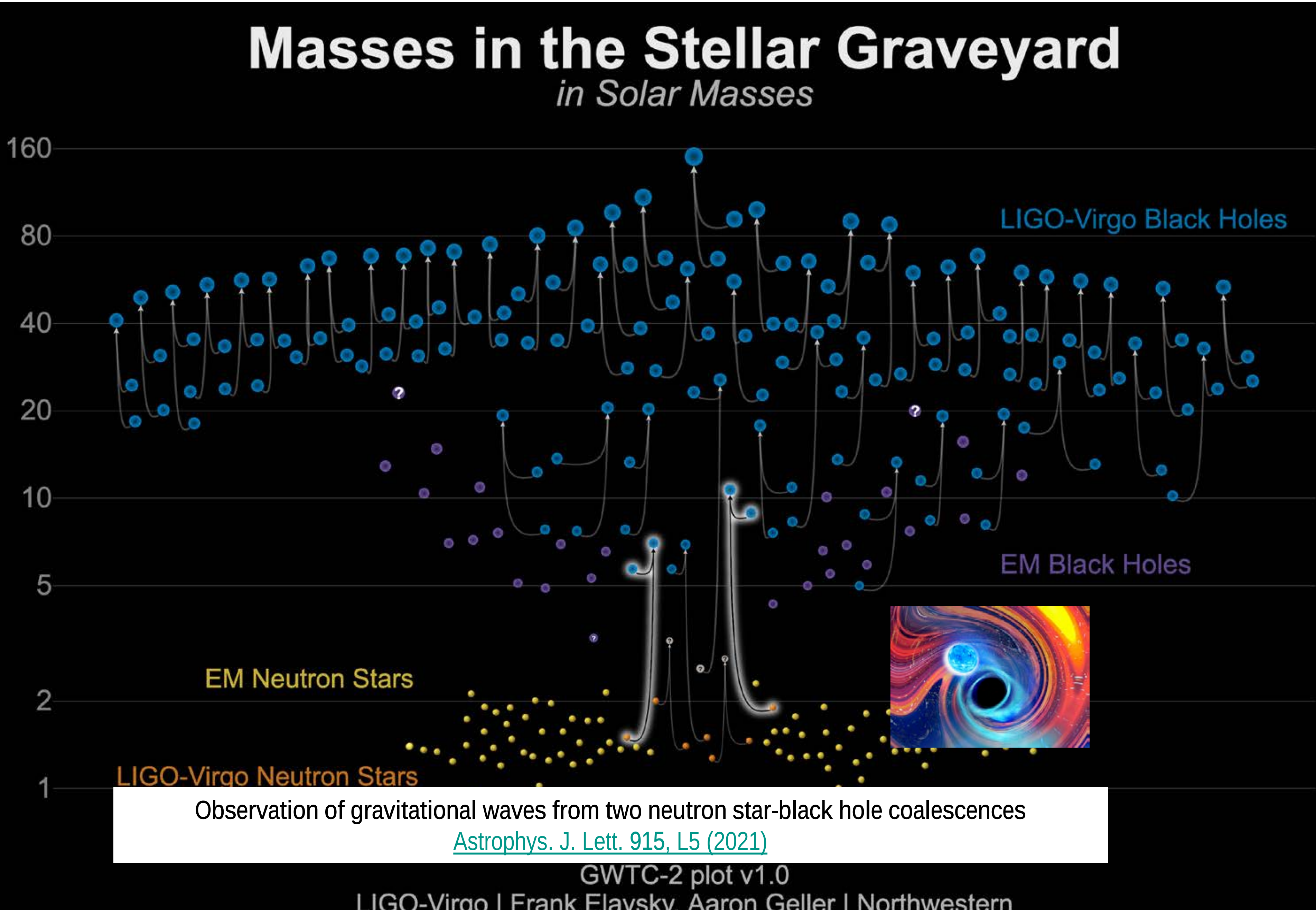

Observation of gravitational waves from two neutron star-black hole coalescences

[Astrophys. J. Lett. 915, L5 (2021)]

Detection Confidence

Phys. Rev. Lett. 116, 061102

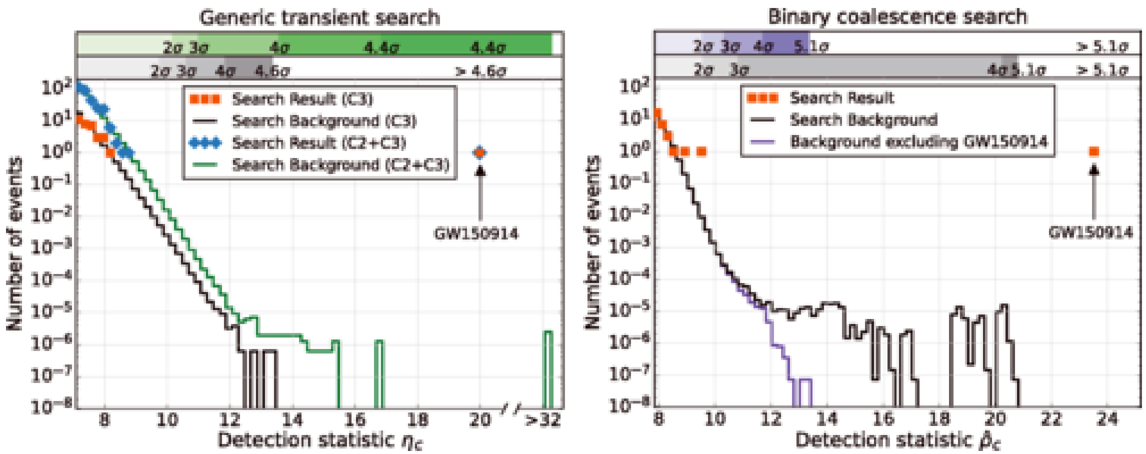

GWTC-1:
Phys. Rev. X 9, 031040 (2019)

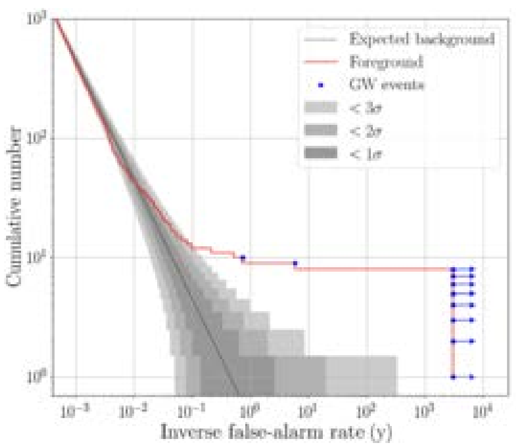

GWTC-2: Phys. Rev. X 11, 021053

Name	Instrument	cWB		GstLAL			PyCBC			PyCBC BBH		
		FAR (yr^{-1})	SNR[a]	FAR (yr^{-1})	SNR	p_{astro}	FAR (yr^{-1})	SNR[a]	p_{astro}	FAR (yr^{-1})	SNR[a]	p_{astro}
GW190408_181802	HLV	$<9.5 \times 10^{-4}$	14.8	$< 1.0 \times 10^{-5}$	14.7	1.00	$<2.5 \times 10^{-5}$	13.5	1.00	$<7.9 \times 10^{-5}$	13.6	1.00
GW190412	HLV	$<9.5 \times 10^{-4}$	19.7	$<1.0 \times 10^{-5}$	18.9	1.00	3.1×10^{-5}	17.9	1.00	$<7.9 \times 10^{-5}$	17.8	1.00
GW190413_052954	HLV	…	…	…	…	…	…	…	…	7.2×10^{-2}	8.6	0.98
GW190413_134308	HLV	…	…	3.8×10^{-1}	10.0	0.95	…	…	…	4.4×10^{-2}	9.0	0.98
GW190421_213856	HL	3.0×10^{-1}	9.3	7.7×10^{-4}	10.6	1.00	1.9×10^{9}	10.2	0.89	6.6×10^{-3}	10.2	1.00
GW190424_180648	L			$7.8 \times 10^{-1\dagger}$	10.0	0.91						
GW190425	LV			$7.5 \times 10^{-4\dagger}$	13.0	…						
GW190426_152155	HLV	…	…	1.4×10^{0}	10.1	…	…	…	…	…	…	…
GW190503_185404	HLV	1.8×10^{-3}	11.5	$<1.0 \times 10^{-5}$	12.1	1.00	3.7×10^{-2}	12.2	1.00	$<7.9 \times 10^{-5}$	12.2	1.00
GW190512_180714	HLV	8.8×10^{-1}	10.7	$<1.0 \times 10^{-5}$	12.3	1.00	3.8×10^{-5}	12.2	1.00	$<5.7 \times 10^{-5}$	12.2	1.00
GW190513_205428	HLV	…	…	$<1.0 \times 10^{-5}$	12.3	1.00	3.7×10^{-4}	11.8	1.00	$<5.7 \times 10^{-5}$	11.9	1.00
GW190514_065416	HL	…	…	…	…	…	…	…	…	5.3×10^{-1}	8.3	0.96
GW190517_055101	HLV	6.5×10^{-3}	10.7	9.6×10^{-4}	10.6	1.00	1.8×10^{-2}	10.4	1.00	$<5.7 \times 10^{-5}$	10.2	1.00
GW190519_153544	HLV	3.1×10^{-4}	14.0	$<1.0 \times 10^{-5}$	12.0	1.00	$<1.8 \times 10^{-5}$	13.0	1.00	$<5.7 \times 10^{-5}$	13.0	1.00
GW190521	HLV	2.0×10^{-4}	14.4	1.2×10^{-3}	15.0	1.00	1.1×10^{0}	12.6	0.93	…	…	…
GW190521_074359	HL	$<1.0 \times 10^{-4}$	24.7	$<1.0 \times 10^{-5}$	24.4	1.00	$<1.8 \times 10^{-5}$	24.0	1.00	$<5.7 \times 10^{-5}$	24.0	1.00
GW190527_092055	HL	…	…	6.2×10^{-2}	8.9	0.99	…	…	…	…	…	…
GW190602_175927	HLV	1.5×10^{-2}	11.1	1.1×10^{-5}	12.1	1.00	…	…	…	…	…	…
GW190620_030421	LV			$2.9 \times 10^{-3\dagger}$	13.1	1.00						
GW190630_185205	LV			$<1.0 \times 10^{-5\dagger}$	15.6	1.00						
GW190701_203306	HLV	5.5×10^{-1}	10.2	1.1×10^{-2}	11.6	1.00	…	…	…	…	…	…
GW190706_222641	HLV	$<1.0 \times 10^{-3}$	12.7	$<1.0 \times 10^{-5}$	12.3	1.00	6.7×10^{-5}	11.7	1.00	$<4.6 \times 10^{-5}$	12.3	1.00

LSU

Detection Confidence

Phys. Rev. Lett. 116, 061102
(GW150914)

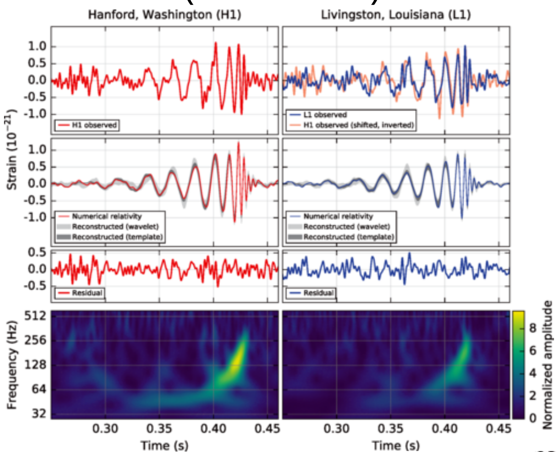

Phys. Rev. Lett. 116, 241103
(GW151226)

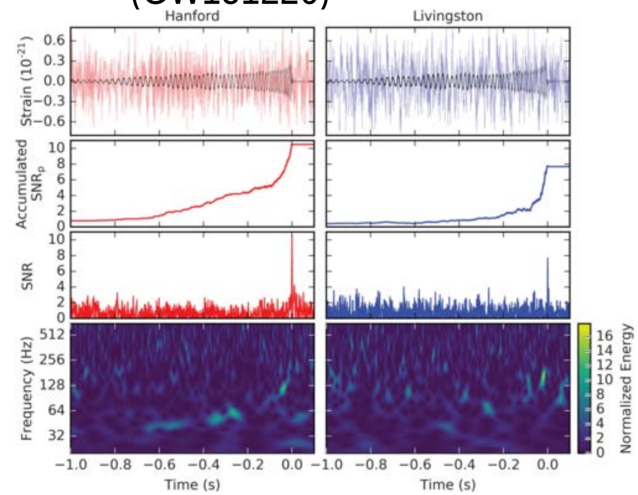

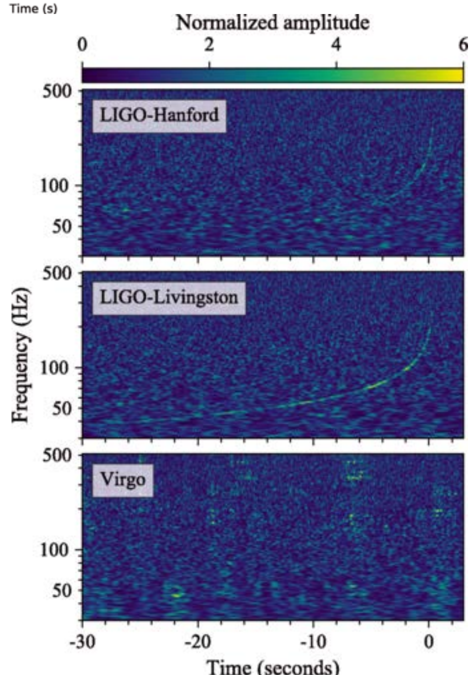

Phys. Rev. Lett. 119, 161101
(GW170817)

O1-O2 (2015-2017)

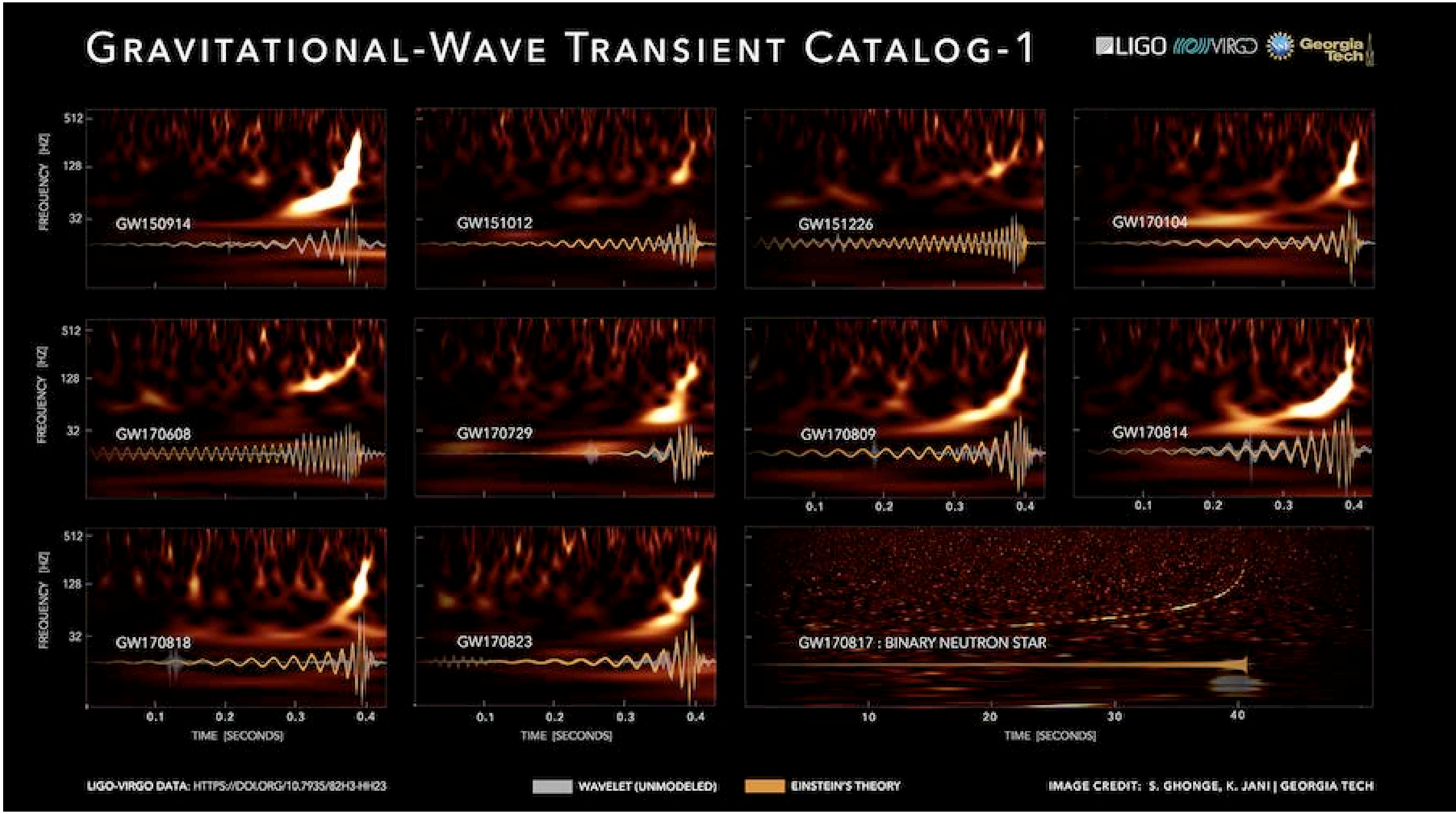

Phys. Rev. X 9, 031040 (2019)

Detection confidence

Phys. Rev. Lett. 119, 161101
(GW170817)

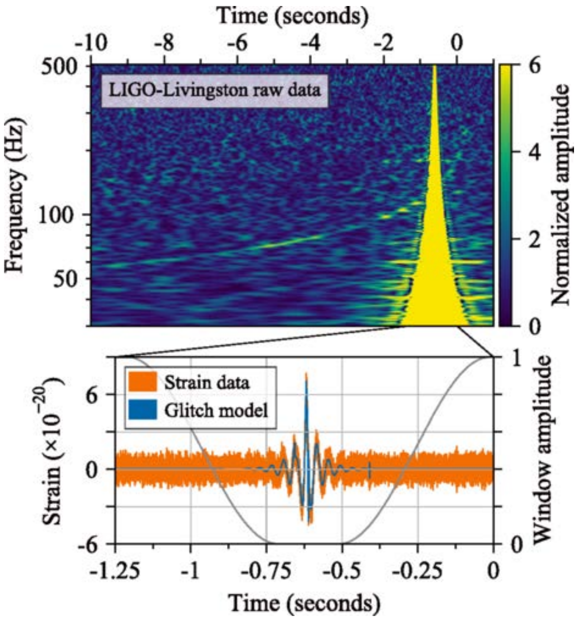

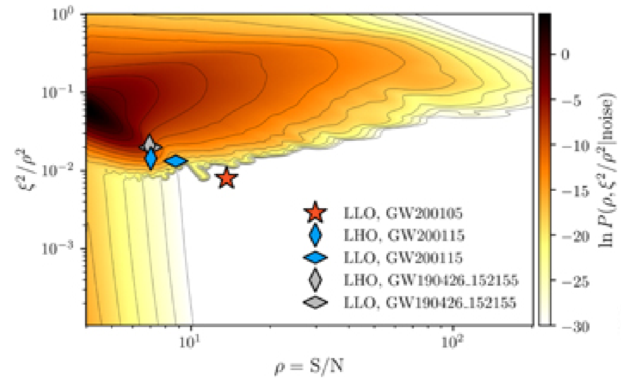

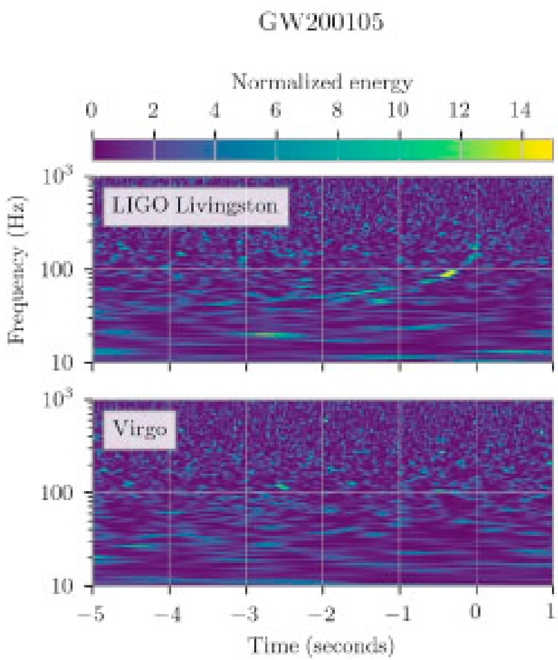

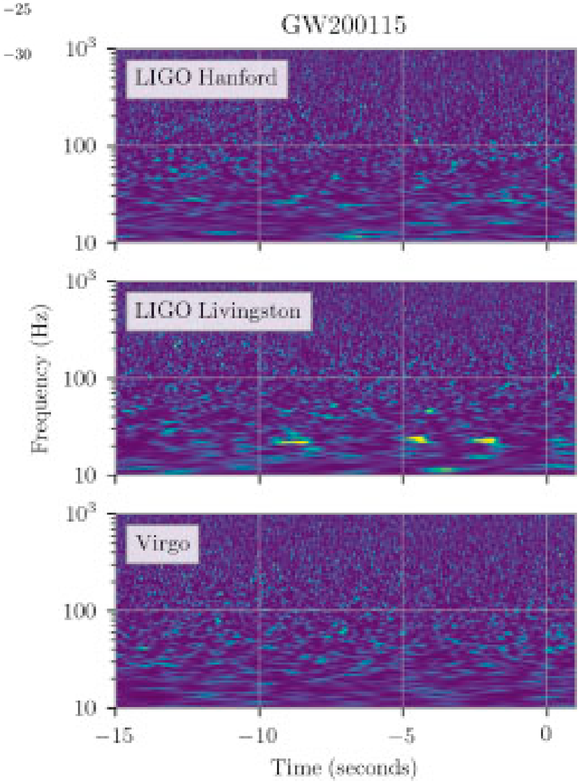

Mass estimates

GWTC-1:
Phys. Rev. X 9, 031040 (2019)

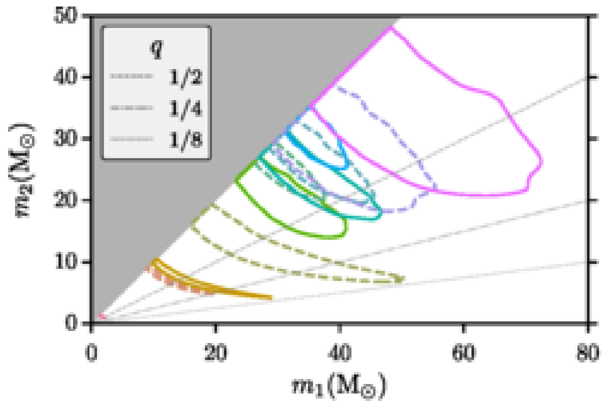

GWTC-2:
Phys. Rev. X 11, 021053

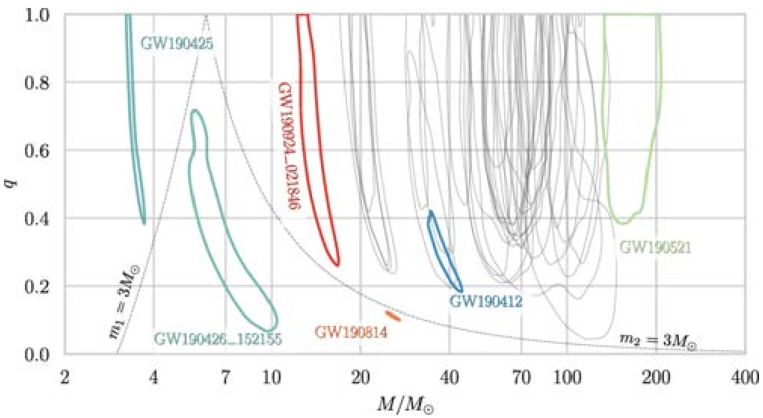

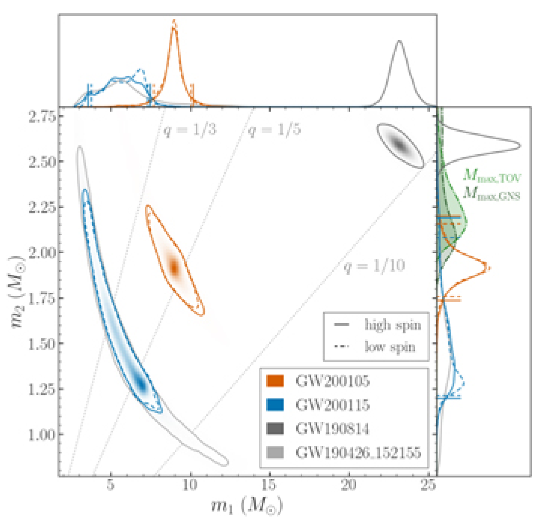

Astrophys. J. Lett 915, L5 (2021)

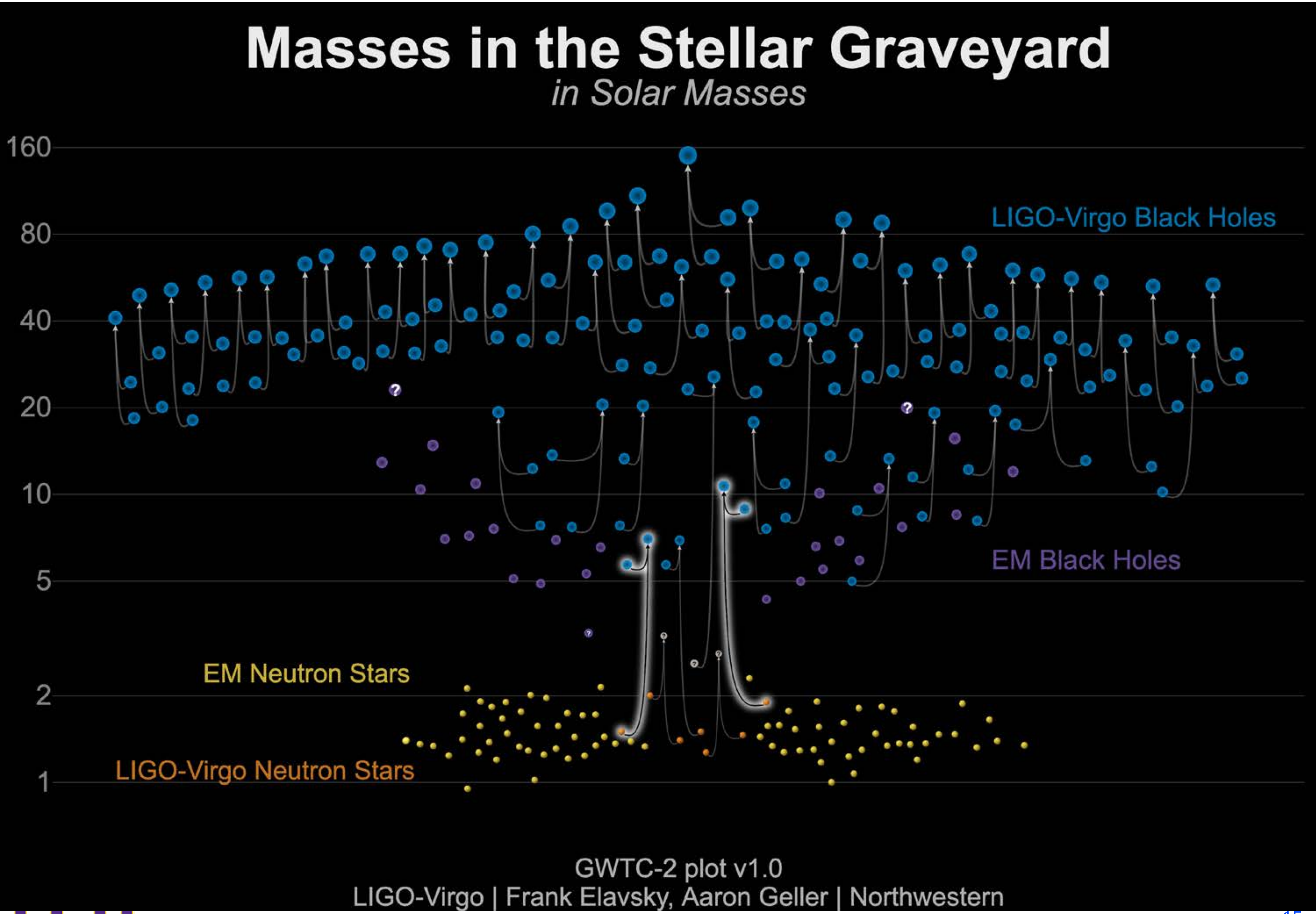
Masses in the Stellar Graveyard
in Solar Masses
160
80
40
20
10
5
2
1
LIGO-Virgo Black Holes
EM Black Holes
EM Neutron Stars
LIGO-Virgo Neutron Stars
GWTC-2 plot v1.0
LIGO-Virgo | Frank Elavsky, Aaron Geller | Northwestern

Localization estimates

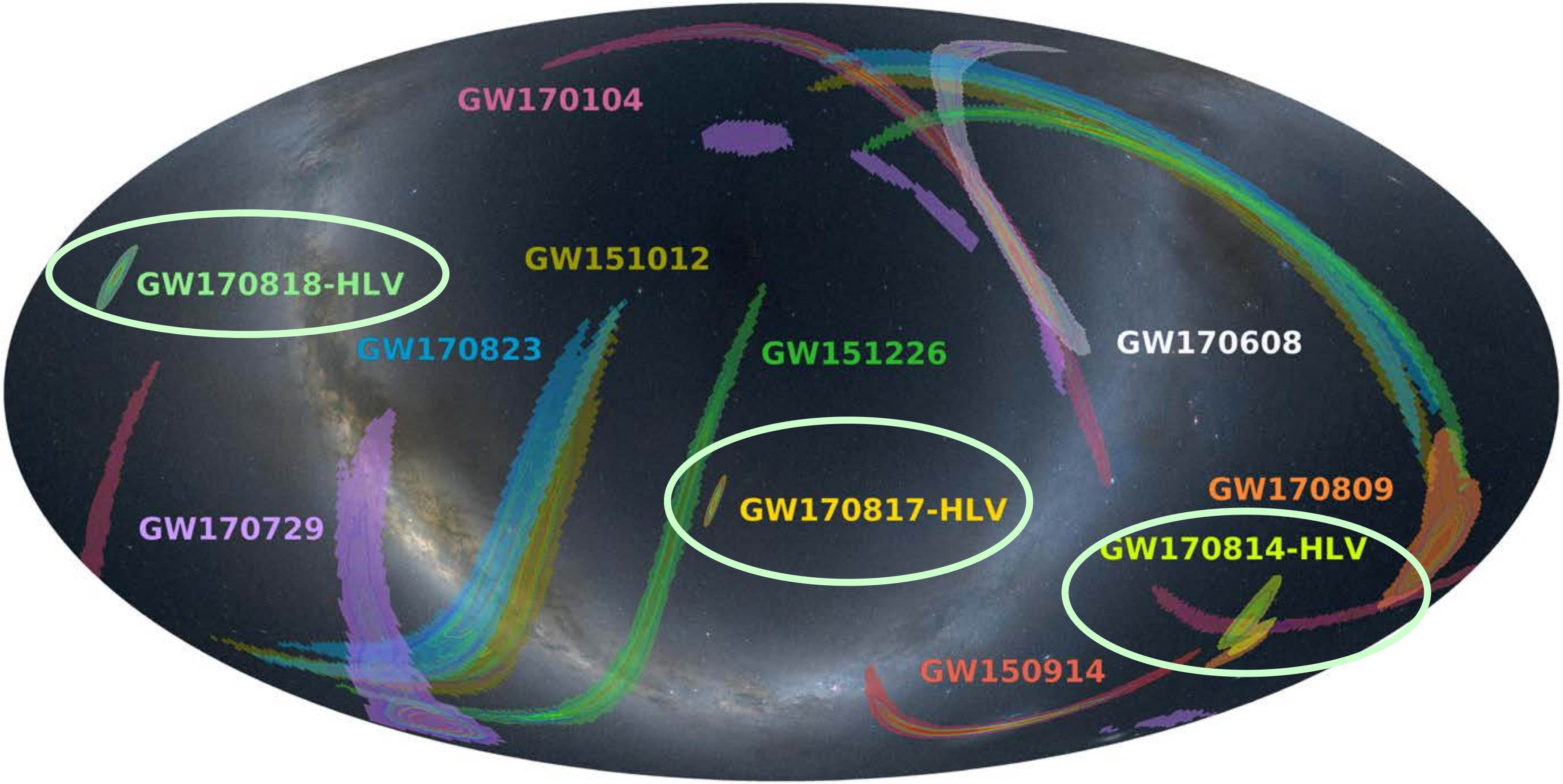

A kilonova rainbow

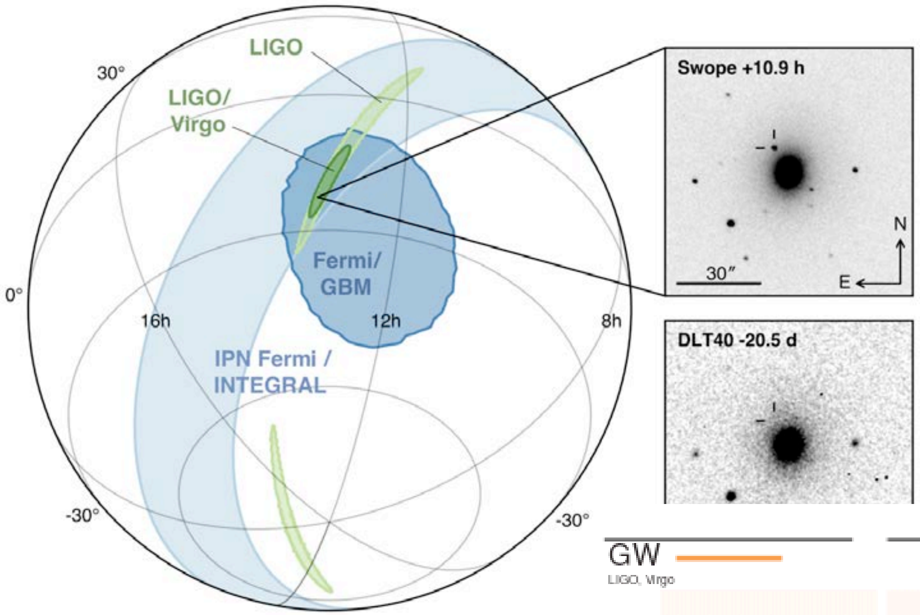

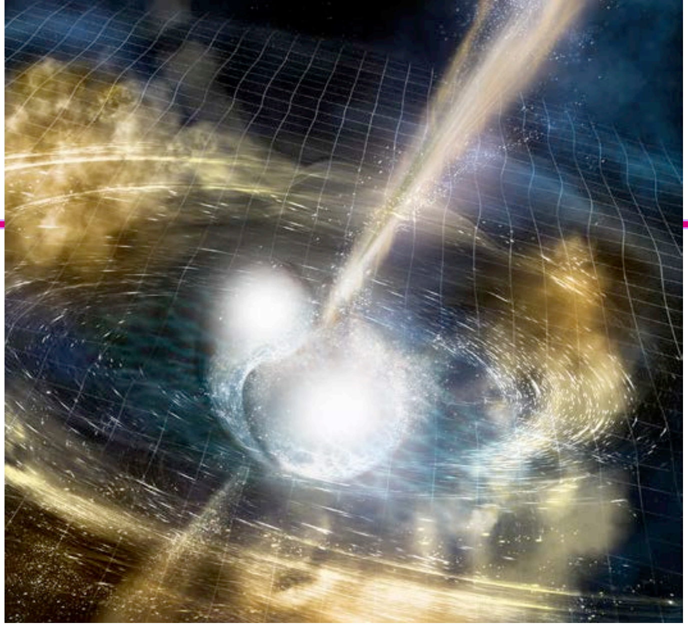

Credit: NSF/LIGO/Sonoma State University/A. Simonnet

Astrophys. J. Lett. 848, L12 (2017)

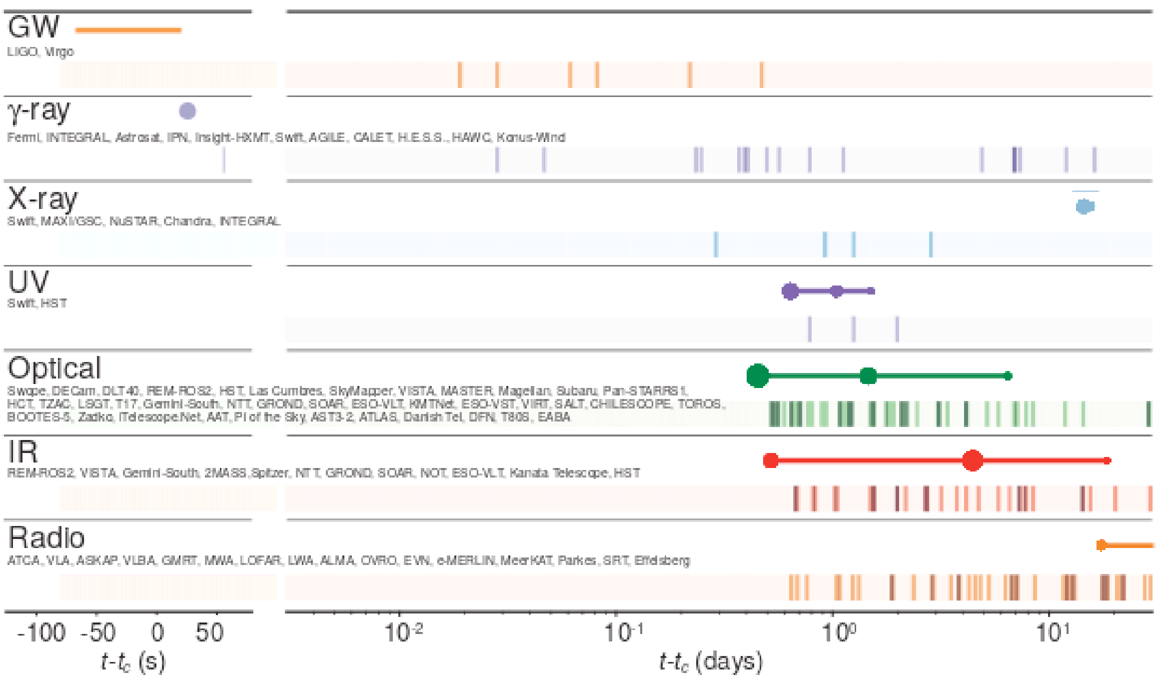

Nuclear physics with GWs

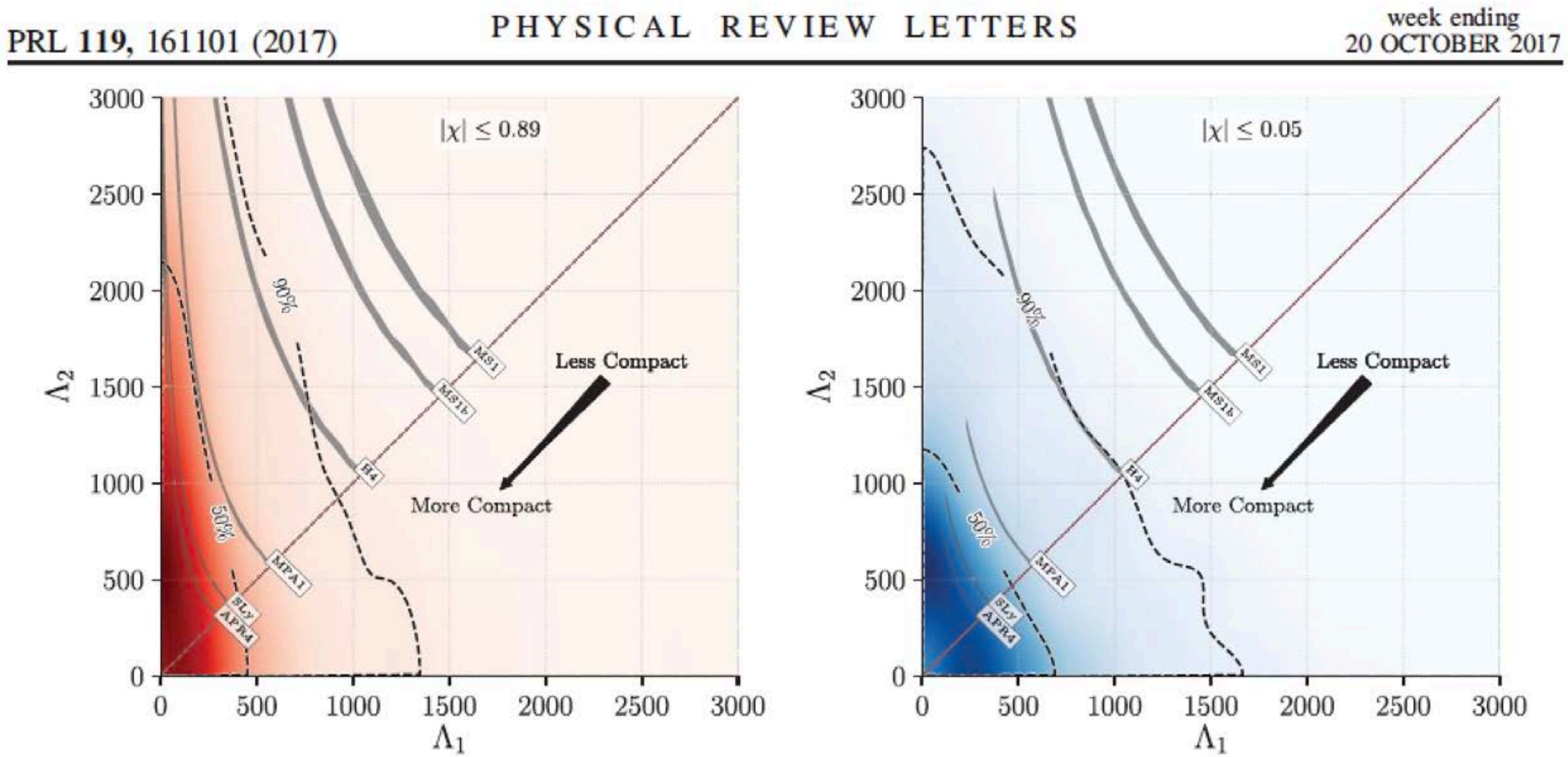

$$\Lambda = \frac{2}{3} k_2 \left(\frac{R}{m} \right)^5$$

GW-GRB observation: Fundamental physics

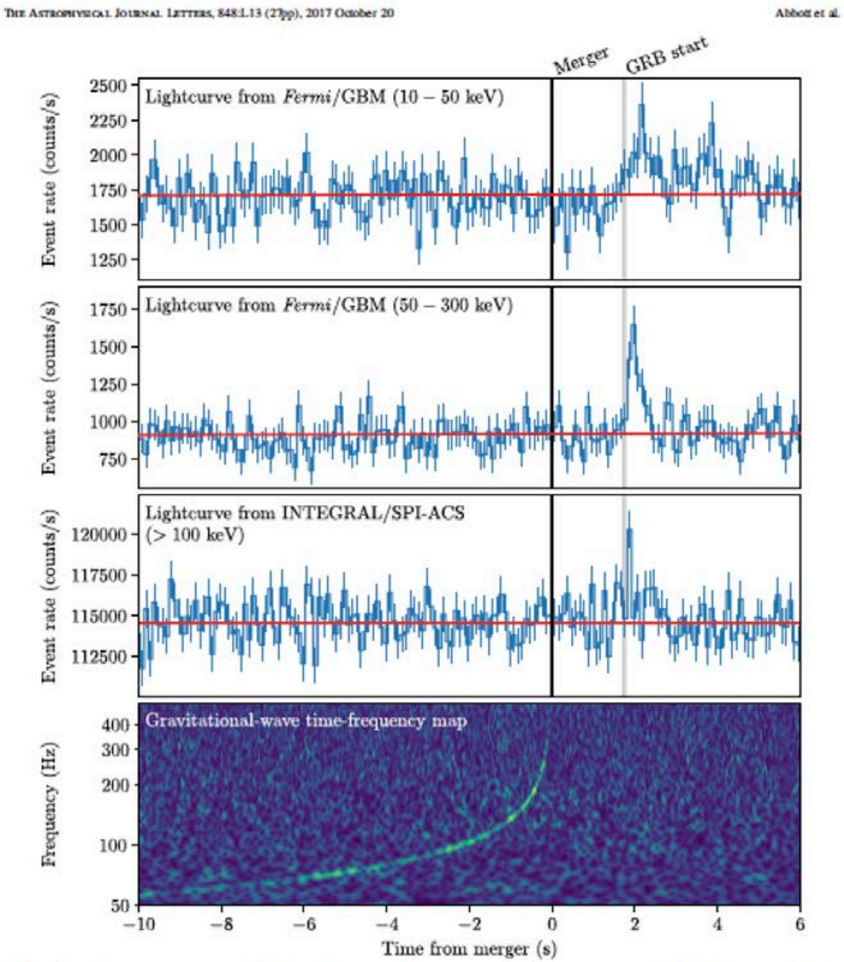

$$-3 \times 10^{-15} \leqslant \frac{\Delta v}{v_{\rm EM}} \leqslant +7 \times 10^{-16}.$$

$$-2.6 \times 10^{-7} \leqslant \gamma_{\rm GW} - \gamma_{\rm EM} \leqslant 1.2 \times 10^{-6}. \quad (4)$$

The best absolute bound on $\gamma_{\rm EM}$ is $\gamma_{\rm EM} - 1 = (2.1 \pm 2.3) \times 10^{-5}$, from the measurement of the Shapiro delay (at radio wavelengths) with the Cassini spacecraft (Bertotti et al. 2003).

ApJL, 848:L13, 2017

Distance estimates

Phys. Rev. Lett. 116, 061102 (GW150914)

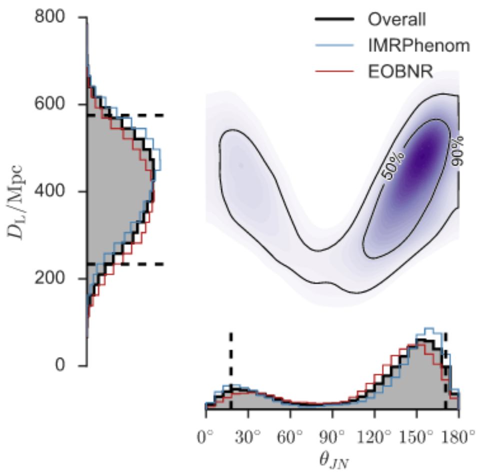

Astroph.J. Lett 915:L5 (2021)

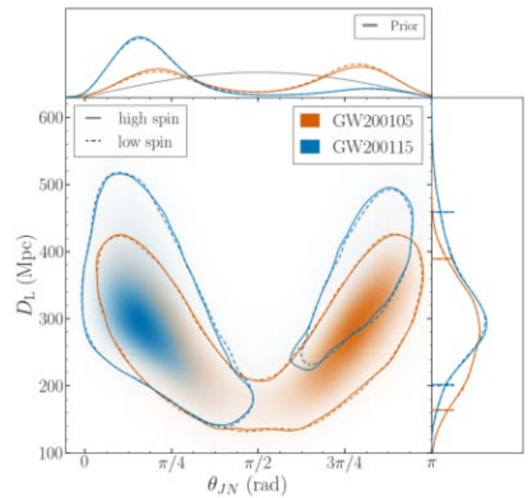

GWTC-1:
Phys. Rev. X 9, 031040 (2019)

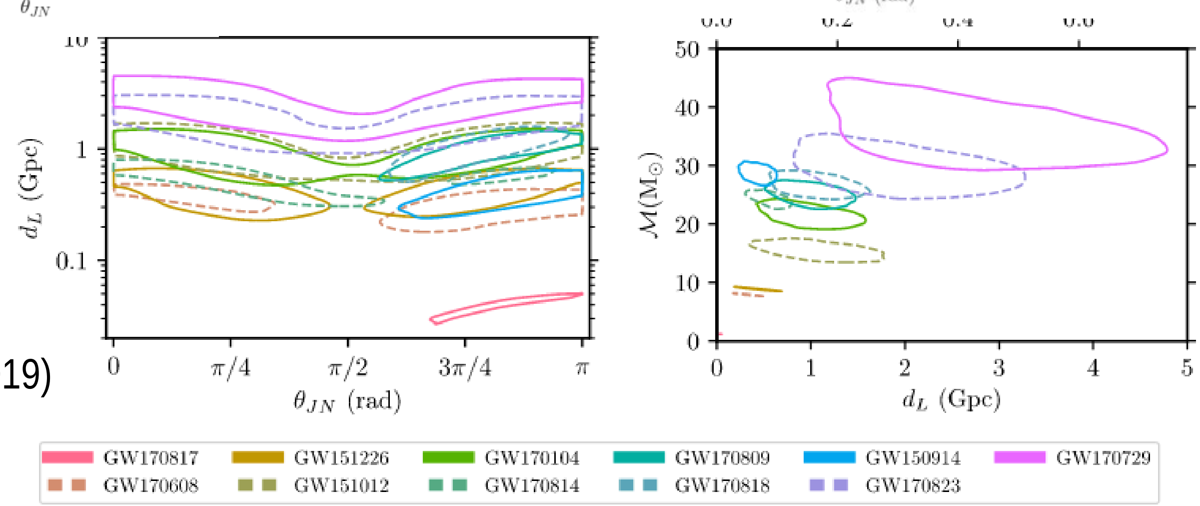

Max distance: GW 4.45 Gpc, GW190413_134308 (chirp mass 33 Ms)

Cosmology with GWs

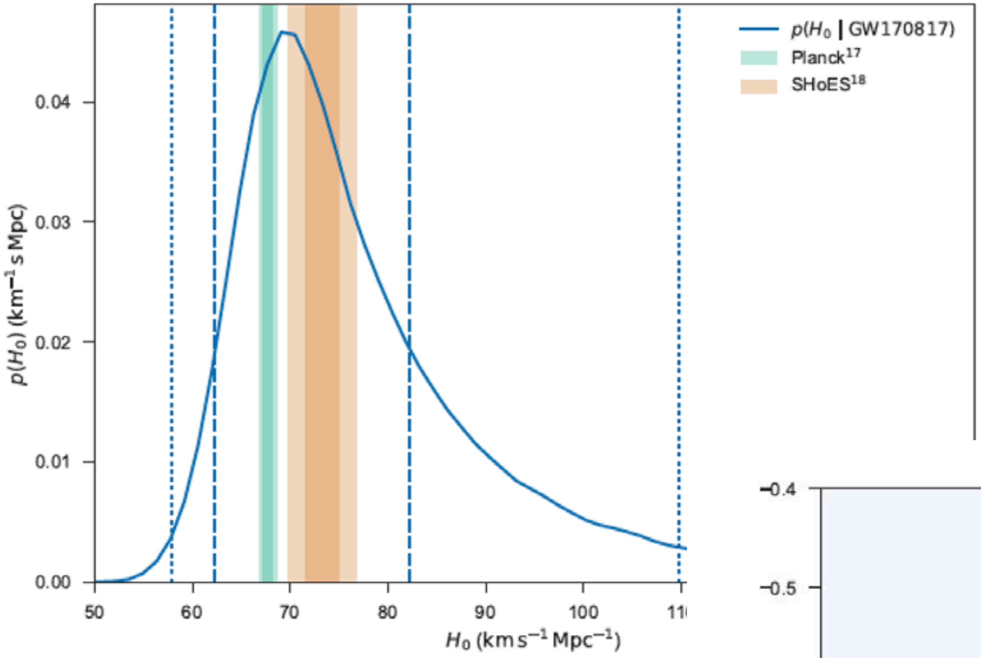

Nature 551, 85 (2017)

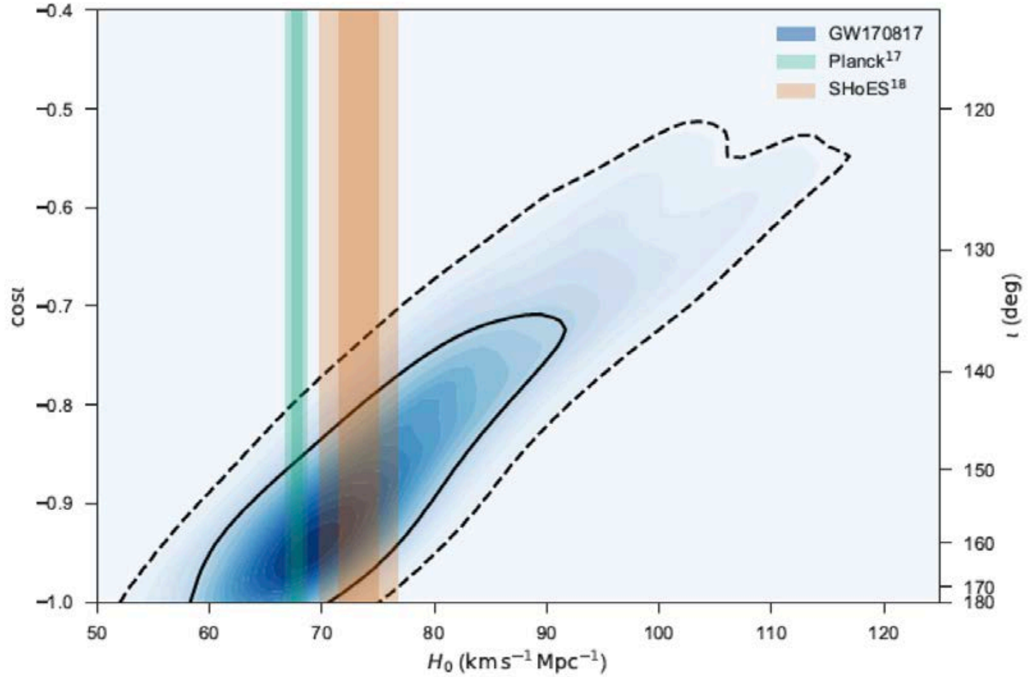

Effective Aligned Spin

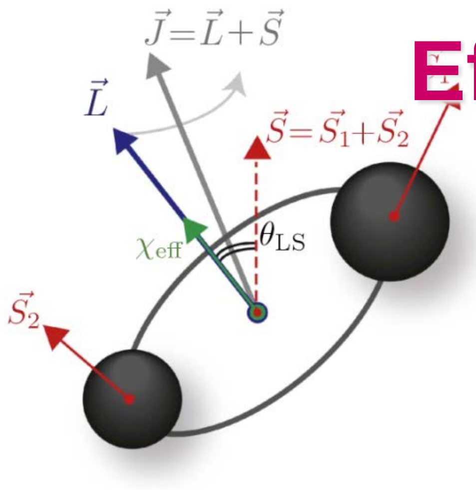

Credit: Carl Rodriguez

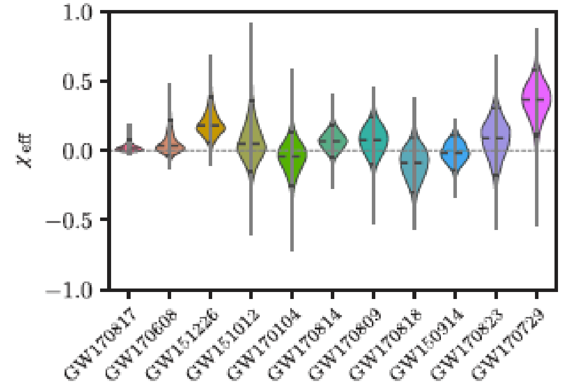

$$\chi_{\rm eff} = \frac{(m_1\vec{\chi}_1 + m_2\vec{\chi}_2)\cdot\hat{L}_N}{M},$$

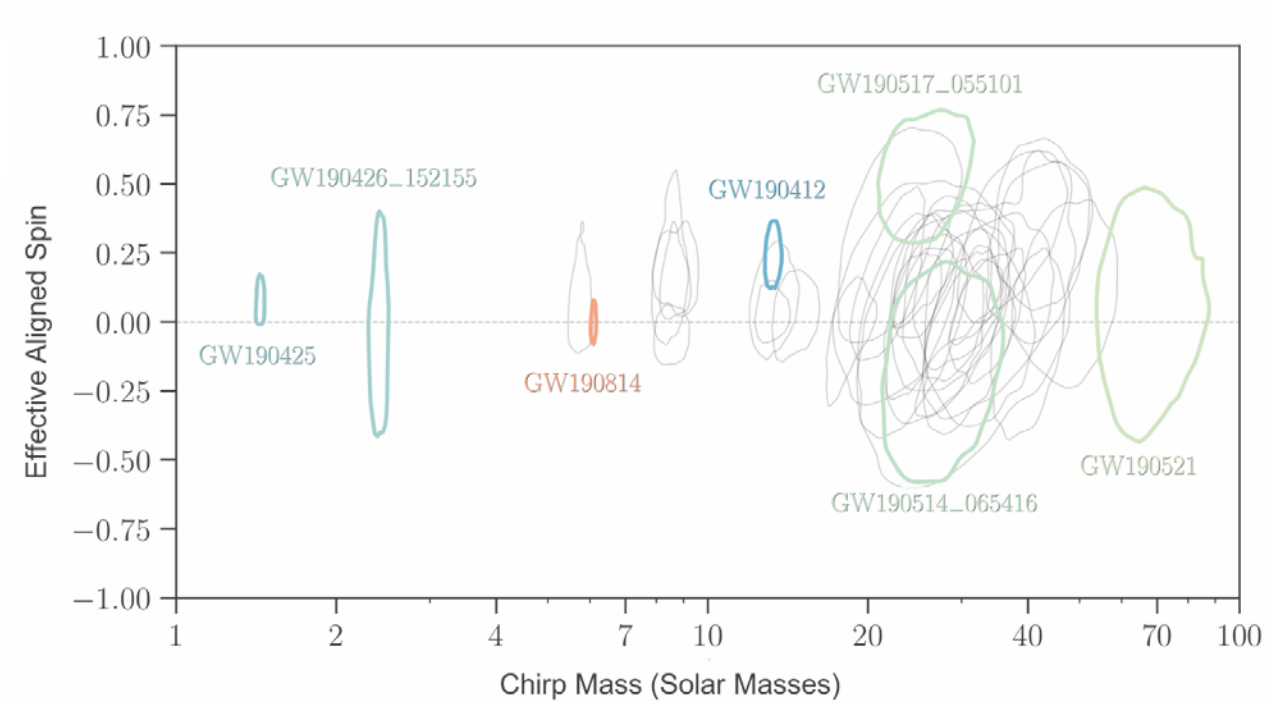

Effective Precession Spin

Credit: LIGO/Caltech/MIT/Son ma State (Aurore Simmonnet)

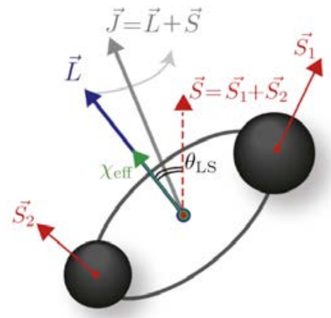

$$\chi_p = \frac{1}{B_1 m_1^2} \max\left(B_1 S_{1\perp}, B_2 S_{2\perp}\right) > 0,$$

$$B_1 = 2+3m_2/(2m_1),\ B_2 = 2+3m_1/(2m_2)$$

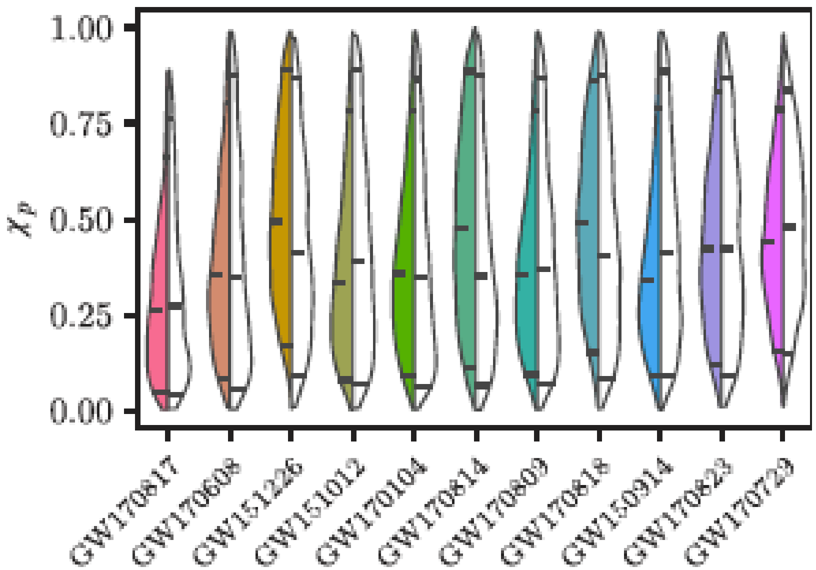

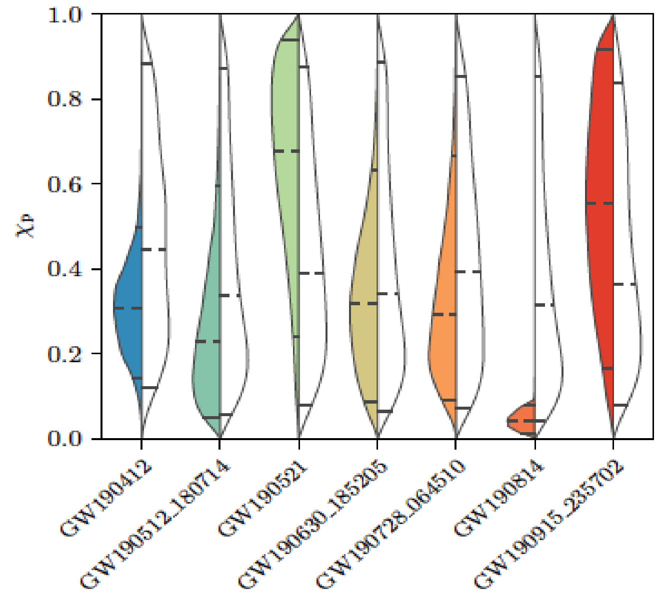

Spin estimates

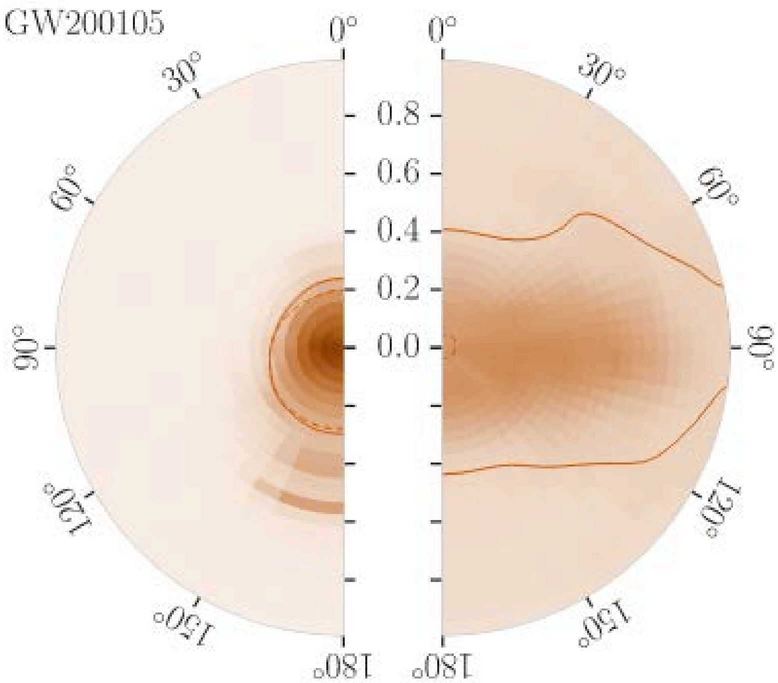

Primary Secondary

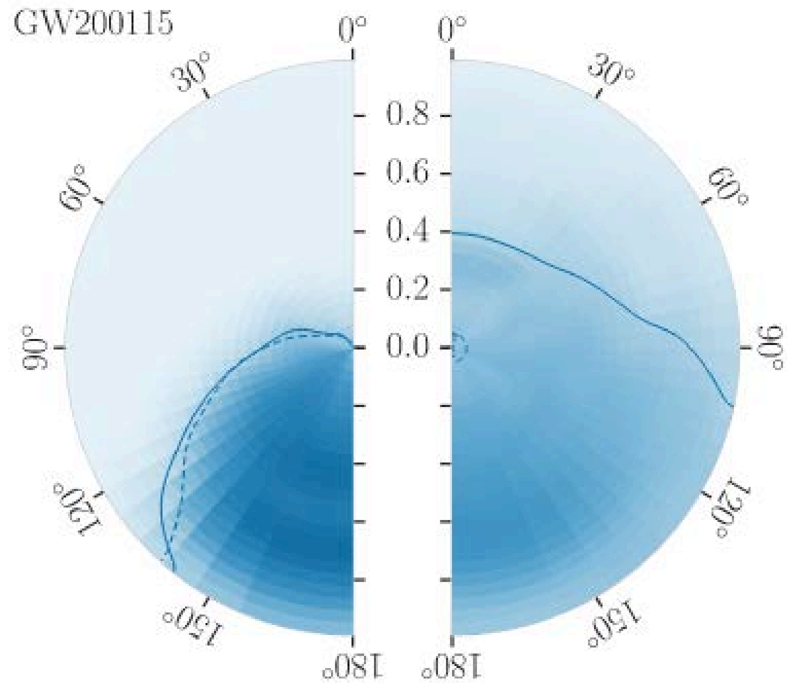

Primary Secondary

Testing General Relativity

Phys. Rev. D 100, 104036 (2019)

SNR	GR tests performed				
	RT	IMR	PI	PPI	MDR
$25.3^{+0.1}_{-0.2}$	✓	✓	✓	✓	✓
$9.2^{+0.3}_{-0.4}$	✓	–	–	✓	✓
$12.4^{+0.2}_{-0.3}$	✓	–	✓	–	✓
$14.0^{+0.2}_{-0.3}$	✓	✓	✓	✓	✓
$15.6^{+0.2}_{-0.3}$	✓	–	✓	✓	✓
$10.8^{+0.4}_{-0.5}$	✓	✓	–	✓	✓
$12.7^{+0.2}_{-0.3}$	✓	✓	–	✓	✓
$17.8^{+0.3}_{-0.3}$	✓	✓	✓	✓	✓
$11.9^{+0.3}_{-0.4}$	✓	✓	–	✓	✓
$12.1^{+0.2}_{-0.3}$	✓	✓	–	✓	✓

- RT: If we subtract the best fit from data, are residuals inconsistent with instrumental noise?
- IMR: Are parameters obtained when fitting the inspiral phase different than those fitting the merger-ringdown phase?
- PI/PPI: If we parameterize the inspiral/post-inspiral phase, do we find deviations from the GR parameters?
- MDR: Do we have evidence of a modified dispersion relation (a.k.a. as graviton mass)?

Ans: $m_g < 10^{-23}$ eV/c^2

Testing General Relativity

Phys. Rev. D 103, 122002 (2021)

Event	Inst.	Properties: D_L [Gpc]	$(1+z)M$ [$M_\odot$]	$(1+z)\mathcal{M}$ [$M_\odot$]	$(1+z)M_f$ [$M_\odot$]	χ_f	SNR	Tests performed: RT	IMR	PAR	SIM	MDR	RD	ECH	POL
GW190408_181802	HLV	$1.55^{+0.40}_{-0.60}$	$55.5^{+3.5}_{-3.8}$	$23.7^{+1.4}_{-1.7}$	$53.0^{+3.2}_{-3.4}$	$0.67^{+0.06}_{-0.07}$	$15.3^{+0.2}_{-0.3}$	✓	✓	✓	✓	✓	✓	✓	✓
GW190412	HLV	$0.74^{+0.14}_{-0.17}$	$44.2^{+4.5}_{-4.6}$	$15.2^{+0.2}_{-0.2}$	$42.9^{+4.6}_{-4.7}$	$0.67^{+0.05}_{-0.06}$	$18.9^{+0.2}_{-0.3}$	✓	–	✓	✓	✓	–	✓	✓
GW190421_213856	HL	$2.88^{+1.37}_{-1.38}$	$108.7^{+15.3}_{-12.4}$	$46.6^{+6.6}_{-6.0}$	$103.9^{+14.1}_{-11.3}$	$0.67^{+0.10}_{-0.11}$	$10.7^{+0.2}_{-0.4}$	✓	✓	✓	–	✓	✓	✓	–
GW190503_185404	HLV	$1.45^{+0.69}_{-0.63}$	$91.6^{+11.2}_{-11.8}$	$38.6^{+5.3}_{-6.0}$	$87.6^{+10.2}_{-10.8}$	$0.66^{+0.09}_{-0.12}$	$12.4^{+0.2}_{-0.3}$	✓	✓	✓	–	✓	✓	✓	✓
GW190512_180714	HLV	$1.43^{+0.55}_{-0.55}$	$45.3^{+3.9}_{-2.8}$	$18.6^{+0.9}_{-0.8}$	$43.5^{+4.0}_{-2.8}$	$0.65^{+0.07}_{-0.07}$	$12.2^{+0.2}_{-0.4}$	✓	–	✓	✓	✓	✓	✓	✓
GW190513_205428	HLV	$2.06^{+0.88}_{-0.80}$	$73.6^{+12.7}_{-6.7}$	$29.5^{+5.6}_{-2.5}$	$70.6^{+11.5}_{-6.7}$	$0.68^{+0.14}_{-0.12}$	$12.9^{+0.3}_{-0.4}$	✓	✓	✓	–	✓	✓	✓	✓
GW190517_055101	HLV	$1.86^{+1.62}_{-0.84}$	$85.4^{+9.6}_{-7.3}$	$35.9^{+4.0}_{-3.4}$	$79.8^{+8.8}_{-6.4}$	$0.87^{+0.05}_{-0.07}$	$10.7^{+0.4}_{-0.6}$	✓	–	✓	–	✓	–	✓	✓
GW190519_153544	HLV	$2.53^{+1.83}_{-0.92}$	$155.1^{+16.7}_{-17.9}$	$65.1^{+7.7}_{-10.3}$	$146.8^{+14.7}_{-15.4}$	$0.79^{+0.07}_{-0.13}$	$15.6^{+0.2}_{-0.3}$	✓	✓	✓	–	✓	✓	✓	✓
GW190521	HLV	$3.92^{+2.19}_{-1.95}$	$269.4^{+39.8}_{-34.6}$	$114.8^{+15.2}_{-17.6}$	$256.6^{+36.6}_{-30.4}$	$0.71^{+0.12}_{-0.16}$	$14.2^{+0.3}_{-0.3}$	✓	–	✓	–	–	✓	✓	✓
GW190521_074359	HL	$1.24^{+0.40}_{-0.57}$	$92.6^{+4.8}_{-5.4}$	$39.8^{+2.2}_{-3.0}$	$88.0^{+4.3}_{-4.8}$	$0.72^{+0.05}_{-0.07}$	$25.8^{+0.1}_{-0.2}$	✓	✓	✓	✓	✓	✓	✓	–
GW190602_175927	HLV	$2.69^{+1.79}_{-1.12}$	$171.8^{+23.2}_{-20.6}$	$72.9^{+10.8}_{-13.7}$	$163.8^{+20.7}_{-18.3}$	$0.70^{+0.10}_{-0.14}$	$12.8^{+0.2}_{-0.3}$	✓	–	✓	–	✓	✓	✓	✓
GW190630_185205	LV	$0.89^{+0.56}_{-0.37}$	$69.6^{+4.2}_{-3.5}$	$29.4^{+1.6}_{-1.5}$	$66.3^{+4.2}_{-3.3}$	$0.70^{+0.05}_{-0.07}$	$15.6^{+0.2}_{-0.3}$	✓	✓	✓	✓	✓	–	✓	–
GW190706_222641	HLV	$4.42^{+2.59}_{-1.93}$	$180.3^{+23.3}_{-27.7}$	$75.1^{+11.0}_{-17.5}$	$171.1^{+20.0}_{-23.7}$	$0.78^{+0.09}_{-0.18}$	$12.6^{+0.2}_{-0.4}$	✓	✓	✓	–	✓	✓	✓	✓
GW190707_093326	HL	$0.77^{+0.38}_{-0.37}$	$23.1^{+1.8}_{-0.5}$	$9.89^{+0.1}_{-0.09}$	$22.1^{+1.9}_{-0.5}$	$0.66^{+0.03}_{-0.04}$	$13.3^{+0.2}_{-0.4}$	✓	–	✓	✓	✓	–	✓	–
GW190708_232457	LV	$0.88^{+0.33}_{-0.39}$	$36.1^{+2.5}_{-0.8}$	$15.5^{+0.3}_{-0.2}$	$34.4^{+2.7}_{-0.7}$	$0.69^{+0.04}_{-0.04}$	$13.1^{+0.2}_{-0.3}$	✓	–	✓	✓	✓	✓	✓	–
GW190720_000836	HLV	$0.79^{+0.69}_{-0.32}$	$24.9^{+5.0}_{-1.2}$	$10.4^{+0.2}_{-0.1}$	$23.7^{+5.2}_{-1.2}$	$0.72^{+0.06}_{-0.05}$	$11.0^{+0.3}_{-0.7}$	✓	–	✓	✓	✓	–	✓	✓
GW190727_060333	HLV	$3.30^{+1.54}_{-1.50}$	$104.4^{+11.9}_{-10.9}$	$44.7^{+5.3}_{-5.7}$	$99.2^{+10.7}_{-9.8}$	$0.73^{+0.10}_{-0.10}$	$11.9^{+0.3}_{-0.5}$	✓	✓	✓	–	✓	✓	✓	✓
GW190728_064510	HLV	$0.87^{+0.26}_{-0.37}$	$23.9^{+5.3}_{-0.7}$	$10.1^{+0.09}_{-0.08}$	$22.7^{+5.5}_{-0.7}$	$0.71^{+0.04}_{-0.04}$	$13.0^{+0.2}_{-0.4}$	✓	–	✓	✓	✓	–	✓	✓
GW190814	LV[a]	$0.24^{+0.04}_{-0.05}$	$27.1^{+1.1}_{-1.0}$	$6.41^{+0.02}_{-0.02}$	$26.9^{+1.1}_{-1.0}$	$0.28^{+0.02}_{-0.02}$	$24.9^{+0.1}_{-0.2}$	✓	✓	✓	–	✓	–	–	–
GW190828_063405	HLV	$2.13^{+0.66}_{-0.93}$	$79.9^{+6.9}_{-5.9}$	$34.5^{+2.9}_{-2.8}$	$75.7^{+6.0}_{-5.2}$	$0.75^{+0.06}_{-0.07}$	$16.2^{+0.2}_{-0.3}$	✓	✓	✓	✓	✓	✓	✓	✓
GW190828_065509	HLV	$1.60^{+0.62}_{-0.60}$	$44.4^{+6.4}_{-4.0}$	$17.4^{+0.6}_{-0.7}$	$42.7^{+6.6}_{-4.2}$	$0.65^{+0.08}_{-0.08}$	$10.0^{+0.3}_{-0.5}$	✓	–	✓	✓	✓	–	✓	✓
GW190910_112807	LV	$1.46^{+1.03}_{-0.58}$	$101.9^{+10.4}_{-7.8}$	$43.9^{+4.6}_{-3.6}$	$97.0^{+9.3}_{-7.1}$	$0.70^{+0.08}_{-0.07}$	$14.1^{+0.2}_{-0.3}$	✓	✓	✓	–	✓	✓	✓	–
GW190915_235702	HLV	$1.62^{+0.71}_{-0.61}$	$78.3^{+8.4}_{-8.1}$	$33.1^{+3.3}_{-3.9}$	$74.8^{+7.9}_{-7.4}$	$0.70^{+0.09}_{-0.11}$	$13.6^{+0.2}_{-0.3}$	✓	–	✓	–	✓	✓	✓	✓
GW190924_021846	HLV	$0.57^{+0.22}_{-0.22}$	$15.5^{+5.7}_{-0.7}$	$6.44^{+0.04}_{-0.03}$	$14.8^{+5.9}_{-0.8}$	$0.67^{+0.05}_{-0.05}$	$11.5^{+0.3}_{-0.4}$	✓	–	✓	✓	✓	–	✓	✓

TABLE I. List of O3a events considered in this paper. The first block of columns gives the names of the events and lists the instruments involved in each detection, as well as some relevant properties obtained assuming GR: luminosity distance D_L, redshifted total mass $(1+z)M$, redshifted chirp mass $(1+z)\mathcal{M}$, redshifted final mass $(1+z)M_f$, dimensionless final spin $\chi_f = c|\vec{S}_f|/(GM_f^2)$, and signal-to-noise ratio SNR. Reported quantities correspond to the median and 90% symmetric credible intervals, as computed in Table VI in [16]. The last block of columns indicates which analyses are performed on a given event according to the selection criteria in Sec. II: RT = residuals test (Sec. IV A); IMR = inspiral-merger-ringdown consistency test (Sec. IV B); PAR = parametrized tests of GW generation (Sec. V A); SIM = spin-induced moments (Sec. V B); MDR = modified GW dispersion relation (Sec. VI); RD = ringdown (Sec. VII A); ECH = echoes searches (Sec. VII B); POL = polarization content (Sec. VIII).

Searches for gravitational waves: not just binary systems!

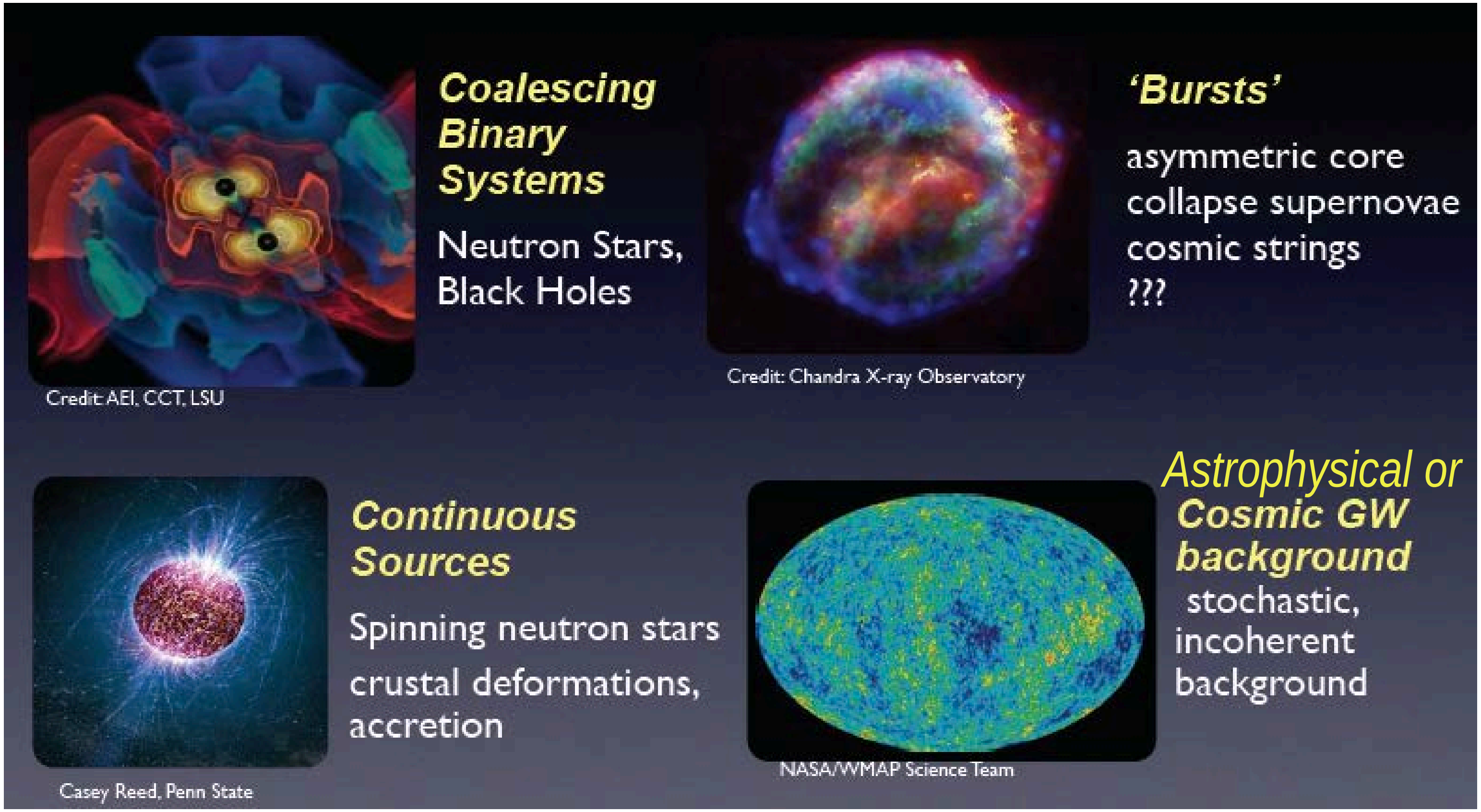

All papers in https://pnp.ligo.org/ppcomm/Papers.html

aLIGO: “Fundamental” noises

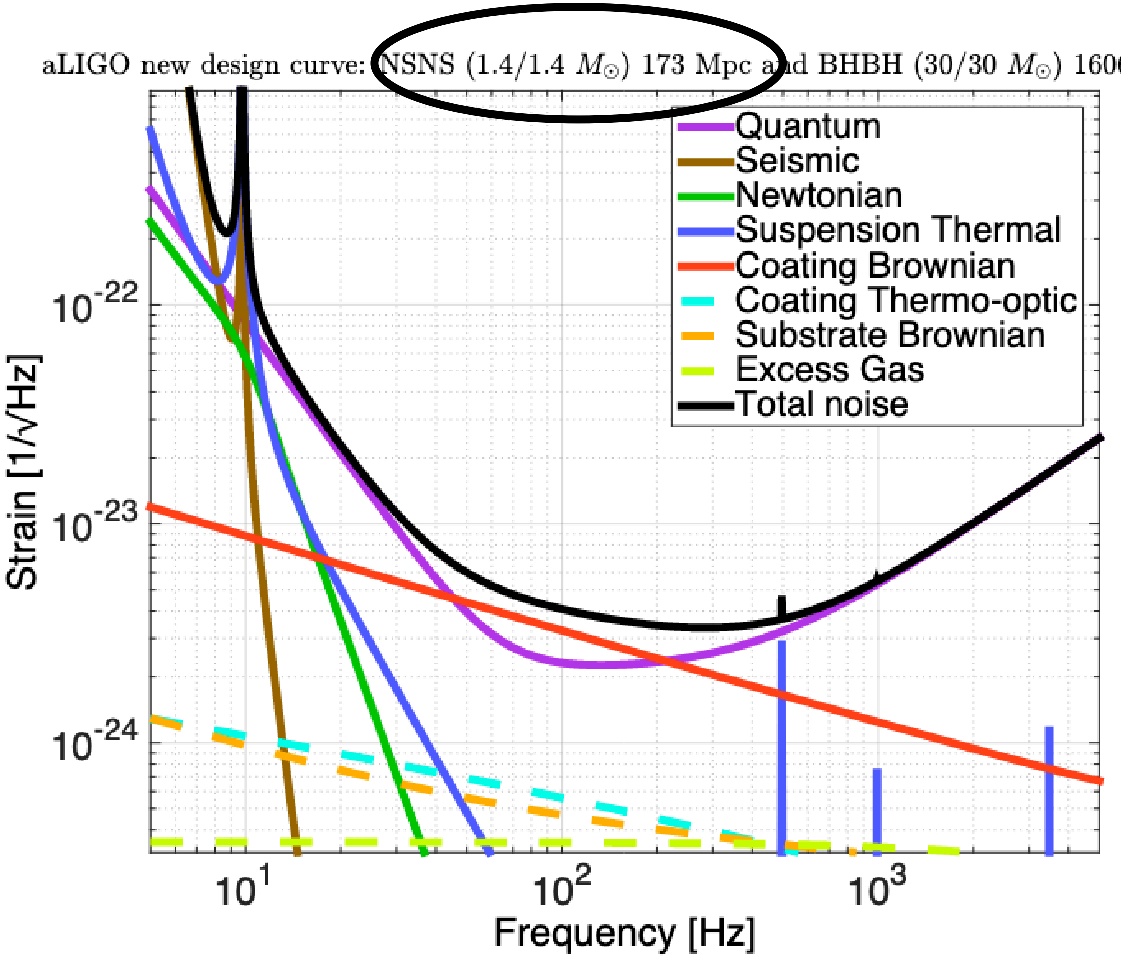

Advanced LIGO: complicated instruments!

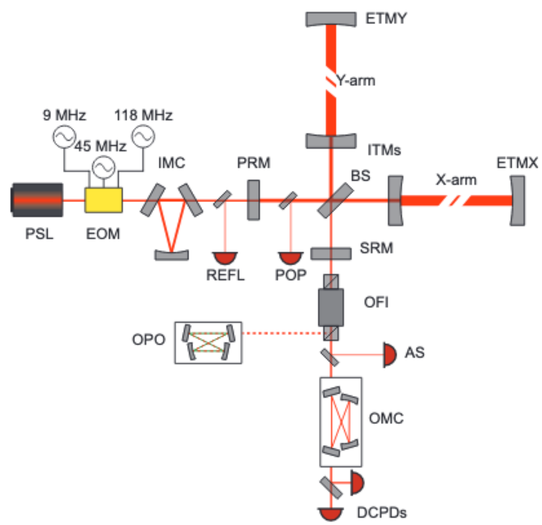

MAX-PLANCK-GESELLSCHAFT

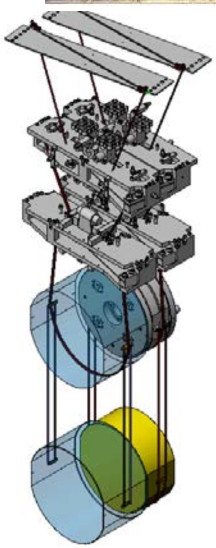

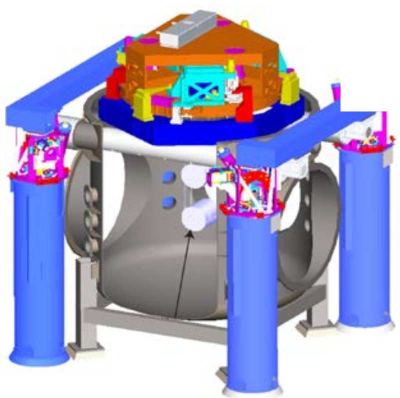

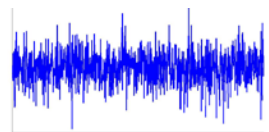

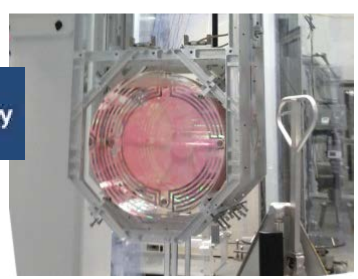

Science & Technology Facilities Council

NSF

LSU

Reducing the noise, increasing the rate of detections

LIGO Livingston Detector

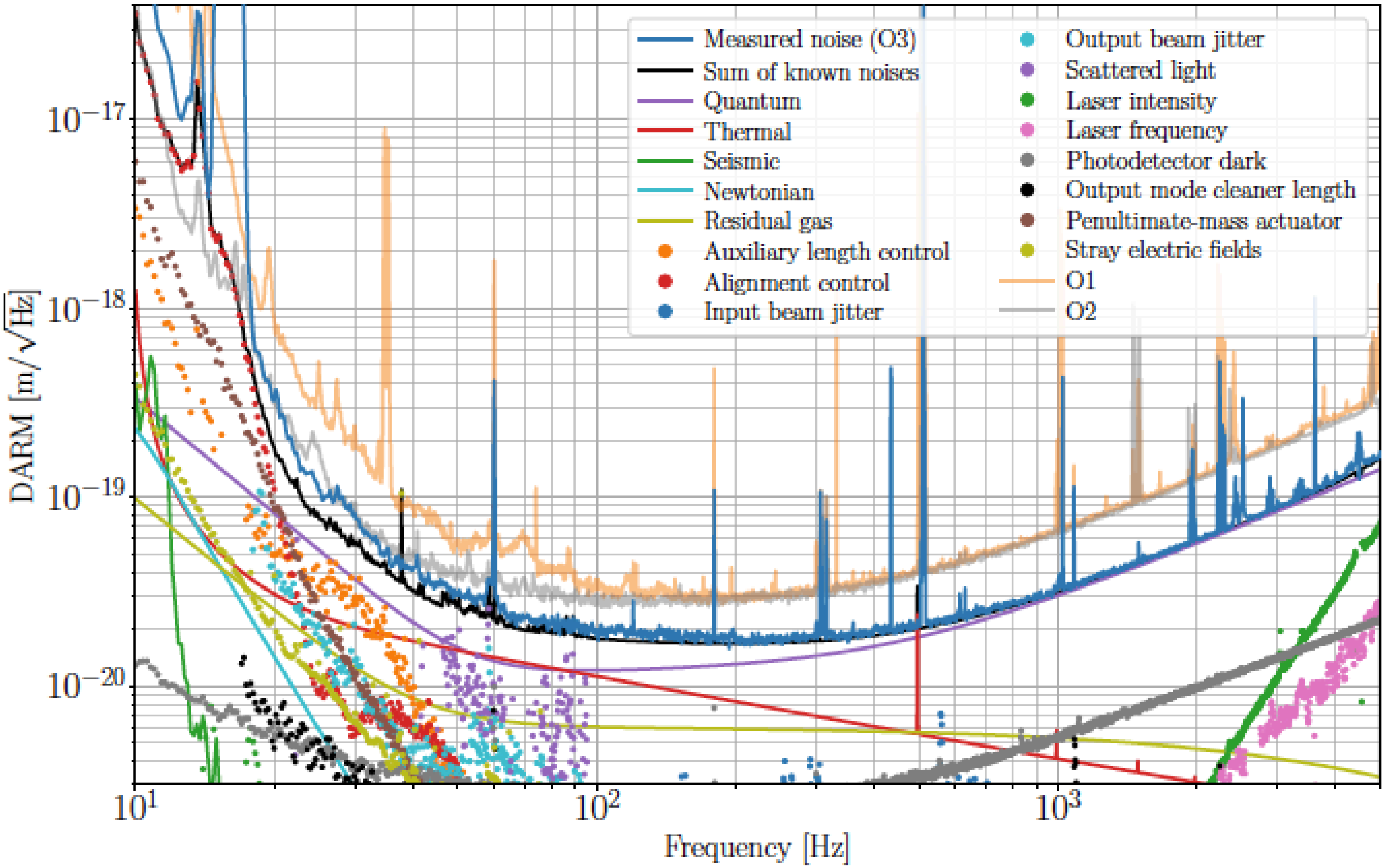

Phys. Rev. D 102, 062003 (2020)

LSU

The next few years

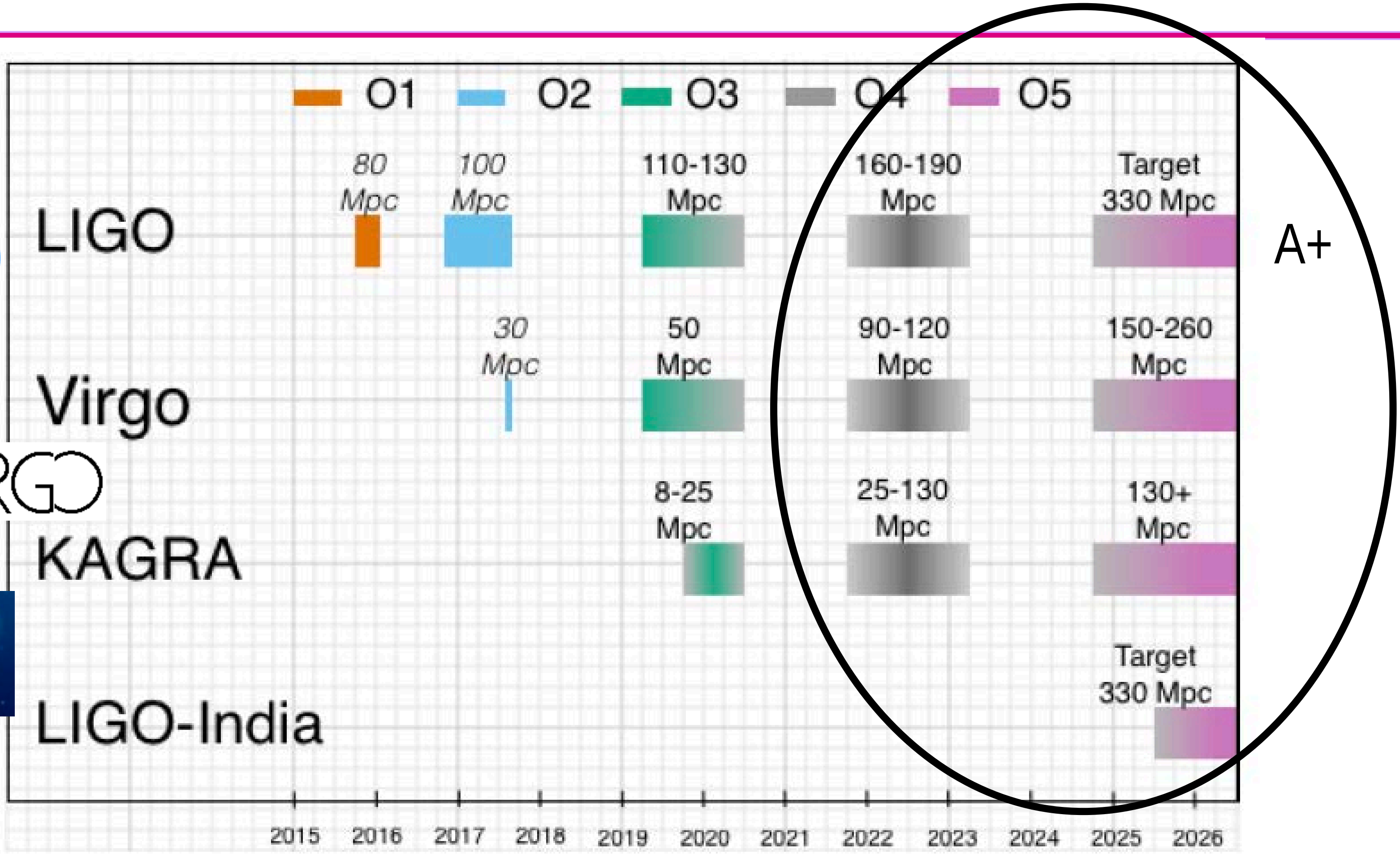

Prospects for Observing and Localizing Gravitational-Wave Transients with Advanced LIGO, Advanced Virgo and KAGRA

https://arxiv.org/abs/1304.0670 (last updated September 2019)

Sensitivities of future detectors

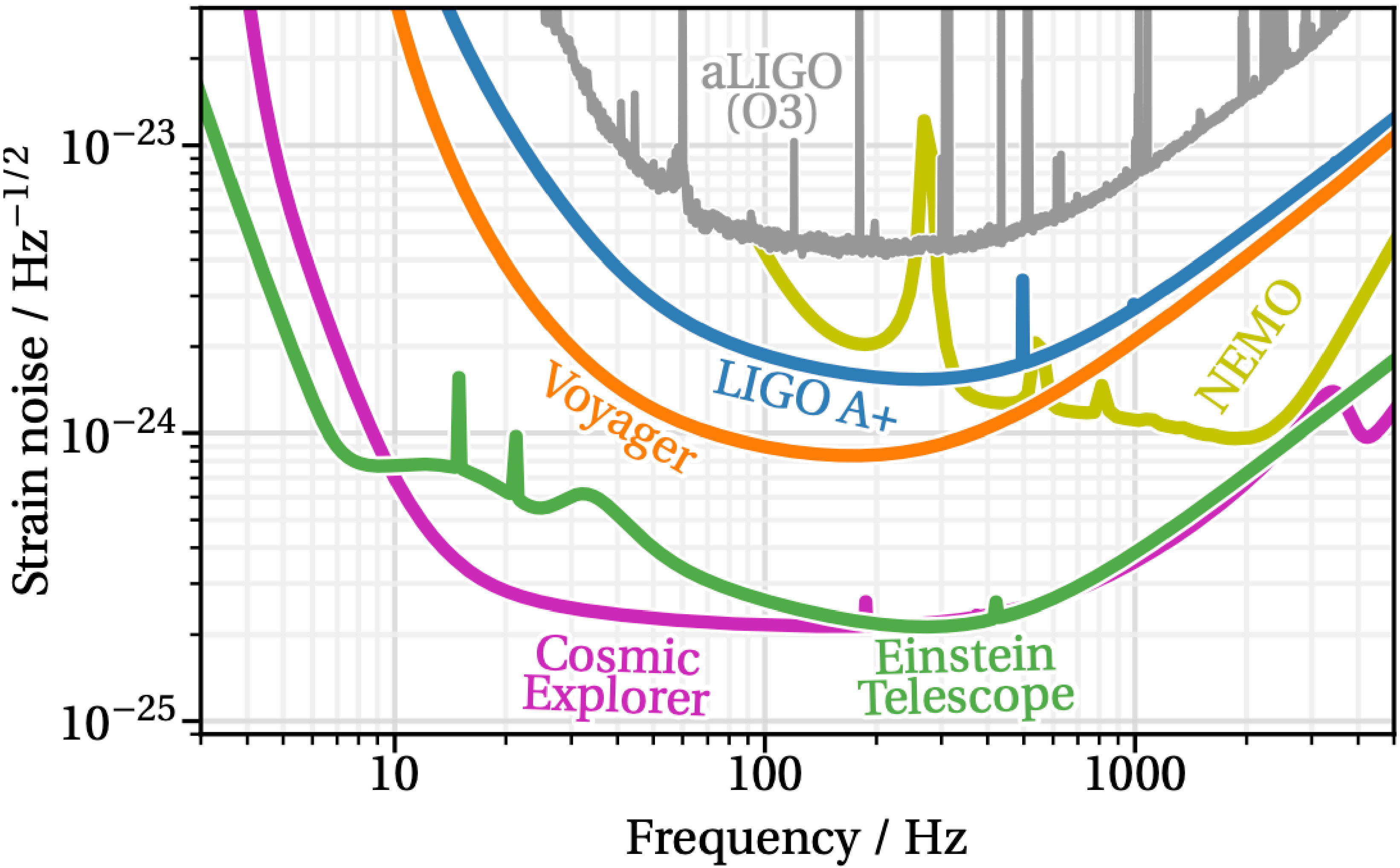

https://cosmicexplorer.org/researchers.html

Third Generation Detectors (Ground based)

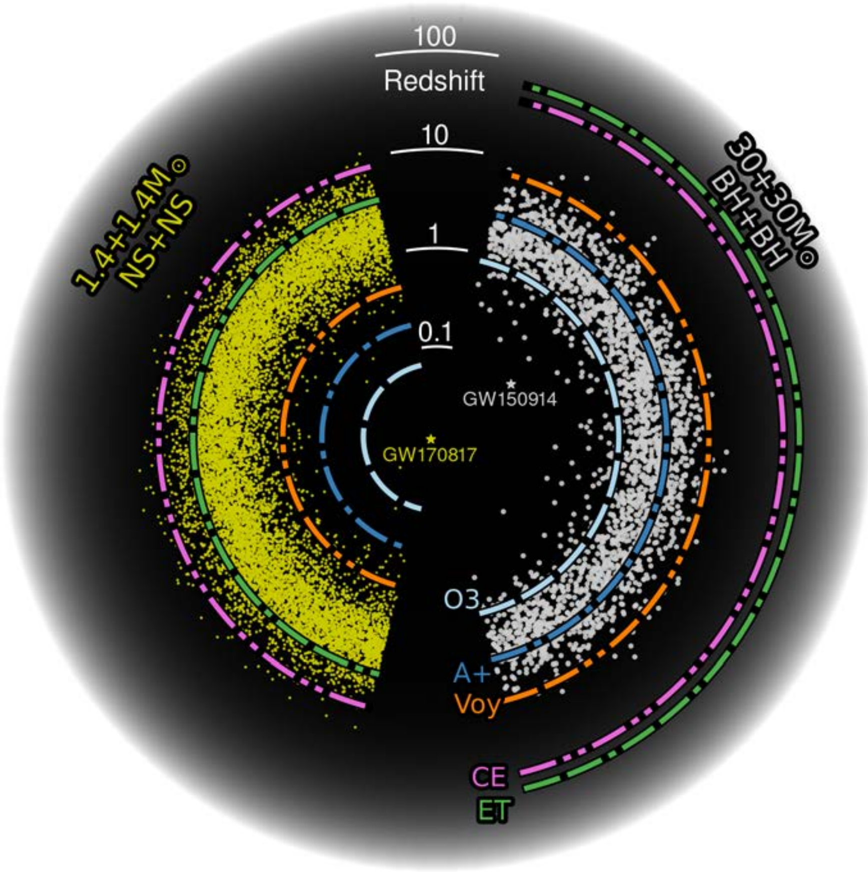

https://cosmicexplorer.org/researchers.html

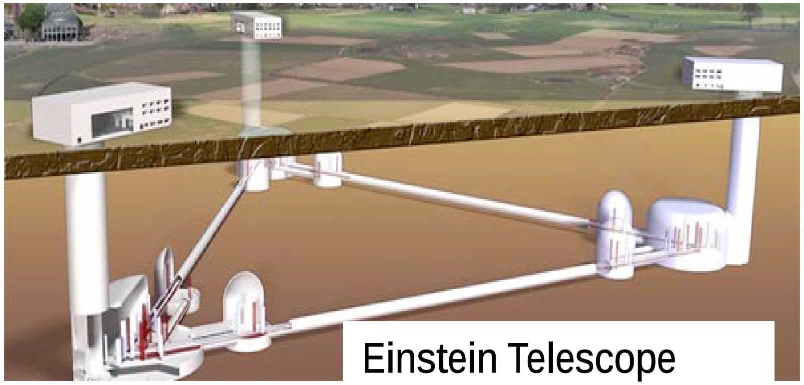

Questions?

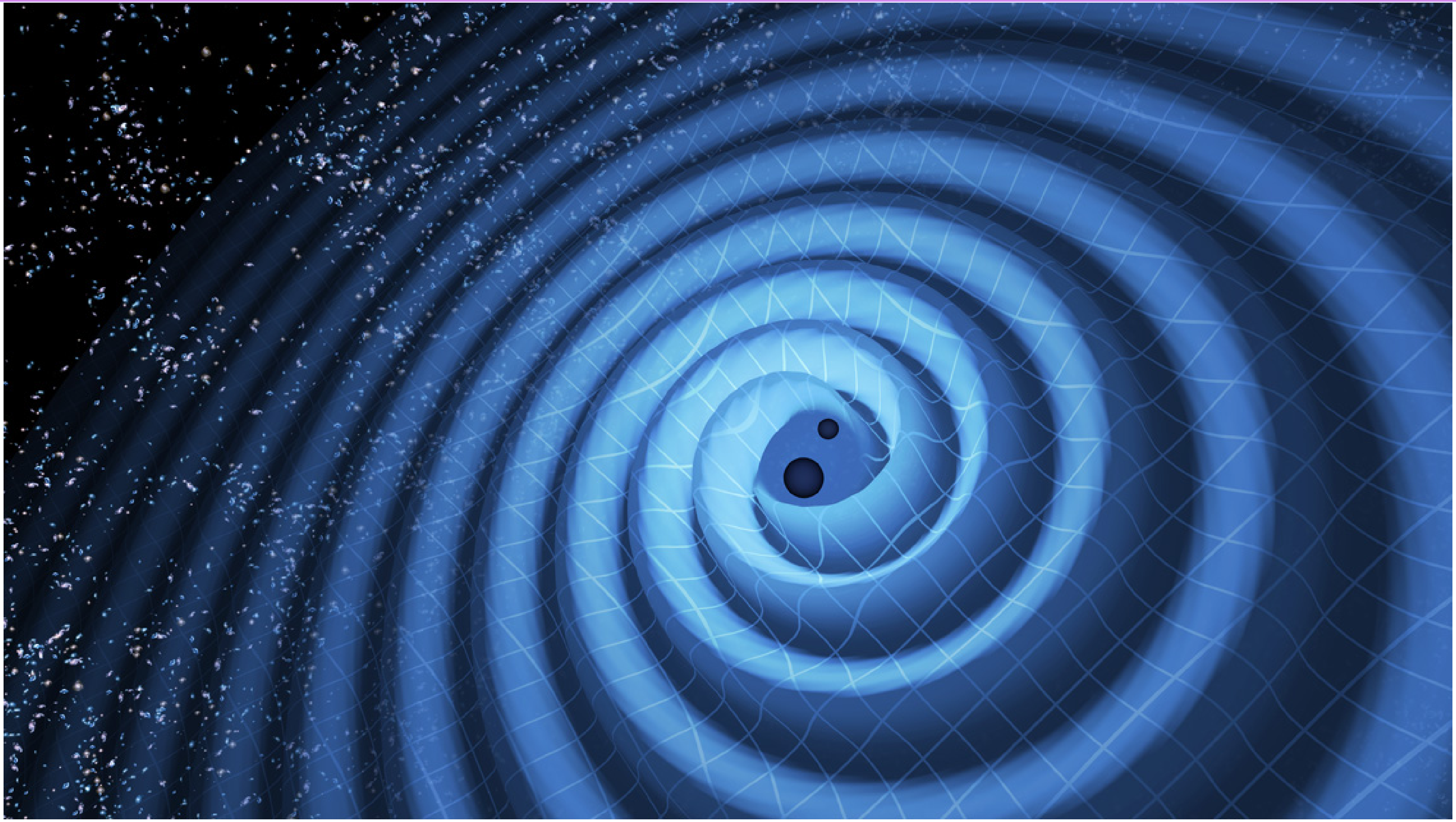

Image credit: LIGO/T. Pyle

www.ligo.org

LSU